NASA TECHNICAL NOTE

NASA TN D-2745

NASA TN D-2745

TORSIONAL VIBRATION CHARACTERISTICS OF A 1/5-SCALE MODEL OF SATURN SA-1

by John J. Catherine

Langley Research Center
Langley Station, Hampton, Va.

NATIONAL AERONAUTICS AND SPACE ADMINISTRATION • WASHINGTON, D. C. • APRIL 1965

TORSIONAL VIBRATION CHARACTERISTICS OF A 1/5-SCALE MODEL OF SATURN SA-1

By John J. Catherine

Langley Research Center
Langley Station, Hampton, Va.

NATIONAL AERONAUTICS AND SPACE ADMINISTRATION

For sale by the Clearinghouse for Federal Scientific and Technical Information
Springfield, Virginia 22151 – Price $3.00

TORSIONAL VIBRATION CHARACTERISTICS OF A 1/5-SCALE MODEL OF SATURN SA-1

By John J. Catherine
Langley Research Center

SUMMARY

The results of a torsional vibration test of a 1/5-scale model of the Saturn SA-1 launch vehicle supported by an eight-cable suspension system simulating a free-free boundary condition are presented herein. The vibration modes, frequencies, and damping were obtained at three weight conditions corresponding to different points in the launch trajectory. These conditions were 100, 48, and 0 percent of the booster propellant load at lift-off. Two values of stiffness of the eight-cable suspension system were employed at the 48-percent weight condition.

The results presented cover the frequency range of 20 to 70 cps and show the unusual frequency spectrum and mode shapes of the Saturn vehicle which result from its clustered configuration. The first torsion mode and a variety of booster modes (modes in which the various outer tanks and engines of the booster stage move relative to each other) are presented. Comparisons, showing good agreement, of the model test results with results from both a full-scale torsional vibration test and a cursory analytical study are also presented.

INTRODUCTION

Several investigations concerning the vibration characteristics of a 1/5-scale dynamic replica model of the Saturn SA-1 vehicle have been conducted at the Langley Research Center. The purpose of these investigations has been to explore the feasibility of using replica models to obtain vibration data which are necessary for the design of complex launch vehicle structures and control systems and also to investigate the vibration properties of clustered tank configurations. Part of these investigations consisted of determining the lateral vibration characteristics of the Saturn model over a range of weight conditions with two different suspension systems (two cable and eight cable). These results are presented in references 1 and 2, respectively. In addition, studies have been made comparing the results shown in references 1 and 2 with results of a ground vibration survey of a full-scale Saturn SA-1 conducted at Marshall Space Flight Center. These studies are presented in reference 3.

In this report, the torsional vibration characteristics of the Saturn model are presented. Torsional resonant frequencies, mode shapes, and damping of the 1/5-scale Saturn are presented for a range of weight conditions simulating flight times of the full-scale vehicle from lift-off to booster burnout. These results were obtained with an eight-cable suspension system and are compared with the results of torsional vibration tests on the full-scale Saturn SA-1 dynamic test vehicle. In addition, the results obtained are compared with an analytical study based on a finite-difference method.

SYMBOLS

f	frequency, cps
G	shearing modulus of elasticity, psi
G_a	gravitational acceleration, 386 in./sec^2
g	damping factor
I	rotational mass moment of inertia, in-lb-sec^2
J	torsional stiffness constant, in.^{4}
L	length, in.
m	mass, lb-sec^2/in.
n	number of cycles used in determining damping
x_o	initial vibration amplitude
x_n	vibration amplitude after n cycles
ρ	mass density, lb-sec^2/in.^{4}

Subscripts:

F	full scale
M	model

DESCRIPTION OF THE 1/5-SCALE SATURN MODEL

The 1/5-scale model of Saturn SA-1 is shown suspended in the vibration test tower in figure 1, and a sketch of the model showing its dimensions and the nomenclature used herein is shown in figure 2. Rotational mass moment of inertia and stiffness distributions were calculated from the known dimensions

and material properties of the model and are presented in figures 3 and 4, respectively. A detailed description of the model is given in reference 1, and only a brief discussion is given herein.

The Saturn model consists of three stages and a conical payload section having an overall length of 388.6 inches (32 ft, 4.6 in.) and a maximum diameter of 52 inches. It weighs about 7400 pounds when ballasted to simulate the lift-off weight condition. Water was used in the model to simulate the mass of the fuel and lox. The model water level was adjusted to obtain the properly scaled total weight.

The principal load-carrying structure of the booster (first stage) consists of a 21-inch-diameter center tank which is firmly attached to the barrel at the lower end and to the spider at the upper end. Eight 14-inch-diameter outer tanks are arranged around the center tank and are attached to the outriggers and the spider beam by two joints at each end of each tank. As with the full-scale design, the four alternating outer tanks have upper joints which can be adjusted to transmit longitudinal loads and thus share the load with the center tank; these tanks are referred to as lox tanks. The other four outer tanks have an upper joint which will not transmit longitudinal loads; these tanks are referred to as fuel tanks.

The first stage is equipped with eight simulated engines. These engines were designed to simulate the center-of-gravity location, total weight, and the moment of inertia about the gimbal point of the full-scale engines. All the engines were rigidly fixed at the gimbal point. No attempt was made to duplicate the mounting of the full-scale engines. The natural frequencies of the engines were determined experimentally and the resulting values are given in table I. Two values of inboard engine frequencies were experienced as a result of a difference in thickness of the torsion beam through which the inboard engines were mounted. (See fig. 5.) An overall view of the torsion beam is shown in figure 6.

The second stage consists of an inner water ballast tank connected to a cylindrical outer shell by means of eight radial truss assemblies. The second stage is attached at the lower end to the second-stage adapter structure only at the junctures of the eight radial trusses with the outer shell. The outer shell then forms the principal structural member of the second stage and supports the weight of the third stage and payload section. The ballast tank which makes up 70 percent of the second-stage weight when water filled is supported within the outer shell structure. The third stage consists simply of a water ballast tank; this tank supports the nose cone weight (including the weight of a simulated payload) of 14 pounds.

The rotational moment of inertia of the individual empty stages about the longitudinal center line was determined experimentally by using a bifilar pendulum method and the results are shown in table II.

APPARATUS

Eight-Cable Suspension System

A close-up view of the Saturn model showing the eight-cable suspension system and the shaker orientation is presented in figure 6. A sketch showing the pertinent suspension system dimensions is shown in figure 7 and a detailed description of the suspension system is given in reference 2. The term "eight-cable" is used as a convenient name for this suspension, the principal feature of which is the support of the model by cables attached at the ends of the eight outriggers.

A parallel bank of six springs was used in series with each cable set for tests at all the weight conditions studied. In addition, with the 48-percent weight condition only, a series of tests were performed with each spring replaced by a rigid $\left(1\frac{1}{2}\text{-inch by }\frac{1}{4}\text{- inch cross section, }2\frac{1}{2}\text{ inches long}\right)$ steel link. For the model tests described herein, these two types of suspension are termed spring suspension and rigid-link suspension, respectively. Turnbuckles in series with the cables were used to distribute the model weight evenly among the eight support points. The total weight and weight distribution were determined from load cells in series with the cables and springs as shown in figure 7.

The springs and cables of the suspension system used in this test were identical with those used in the lateral tests of the model; their spring constants are given in reference 2.

Shaker System

Two electromagnetic shakers having a capacity of 50 vector pounds of force each were used to excite torsional vibration of the model. They were oriented 180° apart driving in the same tangential direction perpendicular to the torsional axis lying in the plane of engines 3 and 7. (See illustration in table I.) Torque was applied through a beam held in place by the mounting of the inboard engines to the barrel assembly of the model at station 20. A close-up view of this attachment is shown in figure 5. The torsion beam had a ballast weight of 90 pounds and a calculated rotational moment of inertia of 43.5 in-lb-sec^2. (Ballast weight simulated the weight of aerodynamic fairings and pipings not included on the model.) The shaker force was obtained by electrically adding the output of load cells at the two shaker locations. A shaker and a load cell attached to the torsion beam is shown in figure 8. The shaker force was multiplied by a moment arm of 29 inches to obtain the driving torque.

The two electromagnetic shakers employed in this investigation were controlled by one oscillator. The shaker amplifiers were operated in phase with each other and were balanced by equalizing the force from each of the two load

cells. The frequency of the excitation force was determined from a counter activated by the oscillator.

Instrumentation

Torsional vibration deflections and damping of the model were determined from strain-gage accelerometers having natural frequencies ranging from 90 to 300 cps and damping of about two-thirds critical damping. The locations of the accelerometers fixed to the model are shown in figure 9. The angular rotation along the center tank and upper stages was determined from the tangential accelerations at the cylindrical surface. Two accelerometers were diagonally located at each station. These accelerometers were mounted with their sensitive axis oriented tangent to the model's cylindrical surface as shown in figure 10. At station 343, the outputs from the two accelerometers were combined electronically so that rotation could be directly recorded. (Transfer function data were obtained by this means.) At the other stations, accelerometer outputs were recorded individually. The angular rotation of the outer tanks, outriggers, and engines relative to the model center line was determined from accelerometers such as are shown in figure 11. All accelerations were recorded on oscillographs. In addition to these fixed accelerometers, an accelerometer provided with a vacuum attachment was used as a portable pickup to determine the direction of motion of the spider beam, booster outer tanks, and engines.

Strain gages were placed on all four booster outer lox tanks to measure static longitudinal load. Four strain gages were placed around the periphery of the midstation of each tank and were used to measure the compressive load resulting from adjustment of the lox-tank upper joints.

PROCEDURE

The model was oriented and centered in the test tower by adjusting the turnbuckles in the suspension system until the model weight was divided as evenly as possible among all eight suspension points. The model's vertical axis was then checked by transit. The lox-tank upper joints were adjusted until the outer lox tanks supported 40 percent of the upper stage weight or 180 pounds per tank. The remaining 60 percent was supported by the booster center lox tank. Pressures of 5 psi and of 10 psi were maintained in the booster outer tanks and in the booster center lox tank, respectively.

For all tests reported herein, the second and third stages of the model were maintained fully ballasted with water, and different vehicle configurations were obtained by varying the water level in the booster. Results were obtained for three weight configurations with the spring suspension and one weight configuration with rigid-link suspension. The measured model weight during these tests is given in the following table. The values do not include the weight of the outrigger attachment links (2.0 pounds each), the cables (5.0 pounds each pair), or the spring bank (23.3 pounds each).

Booster water level, percent full	Simulated flight condition	Measured model weight, lb	
		Spring suspension	Rigid-link suspension
0	Burnout	2415	
48	Maximum dynamic response	4770	4765
100	Lift off	7300	

The water level at the lift-off weight condition is termed 100-percent-full condition; however, the booster tanks were not completely full. The designations of the other weight conditions are given in terms of percent of the lift-off weight. For a given water level, the level of the water was the same in all nine tanks of the booster.

At each weight condition, the torsion rigid-body suspension-system frequency was determined and the results are shown in table III and figure 12.

The approximate frequencies of the model resonances were determined by varying the frequency of the shaker input force from about 20 cps to about 70 cps while recording the outputs of the fixed accelerometers on oscillographs.

Each resonance, thus discovered, whether occurring at the nose cone or in the booster stage, was tuned to maximum response where the frequency, the mode shape, and the damping were recorded. The frequencies and mode shapes were determined from the recordings of the response of the fixed and portable accelerometers. The damping of the model was obtained by cutting the input signal to the shaker at the resonant frequency of interest and recording the output of selected fixed accelerometers on the oscillograph. The amplitudes were read from oscillographs and plotted on semilogarithmic paper with a straight line faired through the points. The damping factor g was obtained from the relation:

$$g = \frac{1}{n\pi} \log_e \frac{x_o}{x_n}$$

where

x_o initial vibration amplitude

x_n vibration amplitude after n cycles

RESULTS AND DISCUSSION

Table III summarizes the torsional resonant frequencies and associated damping obtained for three weight conditions of the 1/5-scale model of

Saturn SA-1 suspended by an eight-cable suspension system. The three weight conditions correspond to different flight times of the full-scale vehicle: booster full, lift-off; booster 48 percent full, maximum dynamic pressure; booster empty, burnout.

The variation of resonant frequencies with booster water level is summarized in figure 12. The frequency-response curves and associated mode shapes for the booster full, 48 percent full, and empty are shown in figures 13 to 18, 19 to 27, and 28 to 31, respectively.

Frequencies, Modes, and Damping

A comparison of the frequency response measured at station 343 at the three weight conditions, shown in figures 13, 19, and 28, indicates a substantial change in the response of the model due to a variation of the water level in the booster. For example, the frequency of the first torsion mode was increased some 53 percent by decreasing the booster water level from a full to an empty weight condition. This large variation of frequency is primarily brought about by an associated change in the rotational mass moment of inertia of the eight radially positioned outer tanks of the booster. The outer tanks are located 18.7 inches from the center of the model and each contains approximately 500 pounds of water at the booster full condition.

Damping values shown in table III were obtained from decay decrements determined for each mode. However, a value of g is presented only for those modes where a clean decay was observed. The factors shown in table III are average values obtained from two or more stations on the model. It is seen that the model damping decreased at the first torsion mode as the booster water level was increased.

The mode shapes are presented following the frequency-response curve associated with a particular weight condition and correspond with the labeled response peaks described on these curves. The tests were plagued with suspension-cable resonances at the high end of the frequency range at the three weight conditions and for this reason many of the response peaks occurring in this area were not analyzed.

A study of the mode shapes presented indicates an array of mode shapes peculiar to the clustered design of the booster and the rigid mounting of the engines. Only a few of the mode shapes obtained are analogous to those of a twisting shaft. (Modes of a twisting shaft are determined by the number of nodal cross sections of the center line.) Two mode shapes were obtained that were comparable in this respect: the rigid body mode and the first torsion mode. In both cases, all the booster tanks rotated in the same direction.

In many of the modes obtained, the booster outer-tank angular rotations are predominately in the opposite direction from the deflections of the center tank. By the convention of reference 1, these modes are termed cluster modes. Other coupled modes were predominately outer-tank and engine modes which were identified by the general shape and magnitude of deflection of the engine and outer-tank components.

The mode shape figures show torsional normalized deflections of the model main structure and typical booster outer fuel and lox tanks. Main structure rotation includes the rotation of the corrugated barrel, the booster center tank, part of the spider structure, the second-stage outer shell, and the third-stage tank. In addition, the deflections of an inboard and an outboard engine with corresponding outriggers are shown. Also, the directions of the outer tanks at a particular model station and of the engines at station 0 are indicated by arrows. (Arrows are omitted where the direction of motion was not discernible.) Many of the modes show a six-point survey of the spider beam measured along the beam paralleling the torsion axis.

Rigid body mode.- The rigid body mode shapes are not presented herein; however, their frequency variation with water level is shown in figure 12. It should be noted that the rigid-body mode shapes were straight lines. The suspension frequency was well below the first torsion frequency of the model as indicated by the ratios of the first torsion frequency to the rigid body frequency. Values of these ratios of 50 and 46.5 were obtained for booster-empty and booster-full configurations, respectively.

First torsion mode.- The first torsional mode shapes for booster full, 48 percent full, and empty are shown in figures 14, 23, and 30, respectively. Each mode shape has a single node within the booster stage. The outer tanks are rotating in phase with the center tank.

First cluster mode.- The first cluster mode shapes for the three weight conditions are shown in figures 15, 26, and 31. There is no node on the main structure; however, the outer tanks are rotating out of phase with the center tank. At the booster 48 percent full and empty weight conditions (figs. 26 and 31, respectively) the flexibility of the spider beam and outriggers has a pronounced influence on this mode shape. The spider beam bends (figs. 26 and 31), and the outriggers appear to be moving out of phase from the main structure (fig. 31). The rotation of the ends of the spider beam is out of phase with the center-line rotation, measured along the beam. Since the outer tanks are positioned 20 inches from the center line on the spider beam and on the outriggers, their motion was faired through these points.

Booster outer-tank and engine modes.- Figure 16 shows the outer-tank second bending mode at 41.6 cps with the booster full. The outer lox tanks are out of phase with the outer fuel tanks. This mode was observed during the lateral vibration test as described in reference 2. A coupled first torsion outer-tank second bending mode at 45.6 cps is shown in figure 17. There is one node on the main structure, and the outer lox and fuel tanks appear to be partially in phase with each other. Figure 18 shows a coupled first torsion-cluster mode occurring at 55.4 cps. The main structure has one node and the outer tanks are out of phase with the center tank.

For the booster-48-percent-full condition, two values of suspension system stiffness were tested. The effect of these suspension system changes on the frequencies and modes of the model were found to be of negligible order. For this reason, the mode shapes associated with the rigid-link suspension system have not been presented in this report; only the mode shapes with the spring suspension are presented. All rigid-link data are shown in table III.

Figure 20 shows a booster mode occurring at 20.8 cps. The outer lox and fuel tank motions are opposite from one another. This mode was also observed in the lateral tests (ref. 2) and was termed a "booster mode." Figure 21 shows an outer lox-tank mode; the main structure has one node. Figure 22 shows a first torsion mode at 29.6 cps; however, this frequency corresponds to the resonant frequency of engine number 4 as shown in table I. Accordingly, the minor peak of the double response peak shown in figure 19 is termed an engine mode.

The mode shapes shown in figures 24 and 25 are characterized by a strong response in the booster stage and by very weak upper-stage motion. Figure 25 shows a mode shape at 50.2 cps possessing features of the first cluster mode; however, the spider beam motion indicates lateral bending of the model center line. Accordingly, this mode is termed a coupled torsion-bending mode. An outer-tank second bending mode coupled with the first torsion mode occurs at 63.1 cps and is shown in figure 27.

The engine response was very strong for many of the modes obtained during this investigation, and, in particular, at the booster empty configuration where it substantially influenced the frequency response measured at station 343. A definite correlation may be observed by comparing the frequencies of the response peaks shown in figure 28 with the outboard engine resonant frequencies shown in table I. The normalized value of engine motion shown in figure 29 illustrates the magnitude of the engine response.

Since the full-scale engine mounting was not duplicated for the model and the engine motion had a definite influence on the model response, an investigation was made to determine the importance of engine attachments. This investigation consisted of bracing the four outboard engines together. The bracing consisted of eight pieces of 3/4-inch o.d. thin-wall steel tubing connecting the upper and lower ends of the four outboard engines together as shown in figure 32. The frequency response obtained at station 343 with the engines braced and the booster empty is shown in figure 33. The effect of altering the engine attachment can be seen in figure 33; not only were coupled modes and peaks eliminated, but the magnitude of the first torsion response was also increased by about 200 percent with a 10-percent decrease in the frequency of the peak.

The mode shapes associated with the braced engines are shown in figures 34 and 35. The principal effect of restricting the engine motion was to produce larger amplitudes of the main structure and to contain the response of the engines within the overall range of response of the model.

This study indicates the importance of properly scaling engine supports in order to define adequately model response characteristics.

Nonlinear Studies

The variation of torsion deflection and resonant frequency at station 343 with torque input is shown in figure 36 for outer-tank compressive force values of 0, 900, 1800, and 3600 pounds with the booster full. These values were

obtained by varying the shaker frequency with a given torque input until maximum deflection of the first response peak occurred. Figure 36(a) shows that model deflection is not a linear function of torque input and that for a given value of torque input, the amplitude increases with an increase in the outer-tank compressive force. However, the amplitude does not appear to increase with an increase of compressive force above 1800 pounds (total upper-stage weight). Figure 36(b) shows that frequency decreases with an increase in torque input but shows little variation with increasing outer-tank compressive force.

A similar test was performed with the booster 48 percent full. However, a double response peak was experienced at the first torsion response, as shown in figure 19 (the small response peak corresponds to the natural frequency of engine number 4), and the linearity studies were performed on both peaks. These results are shown in figure 37. Figure 37(a), deflection measured at station 343 at the minor response peak, indicates the same type of nonlinearity as obtained with the booster full with the exception that the response flattened out beyond certain torque levels which increased as the outer-tank compressive load decreased. The response remained flat with an increase in torque input until the major response peak was reached. Also, the frequency decreased with an increase in torque input and increased at a given torque input with an increase of compressive force in the outer tanks as shown in figure 37(c). At the major response peak, the results obtained are contrary to those previously obtained. Figure 37(b) indicates that the model deflection is a linear function of torque input. Also, figure 37(d) shows that the frequency decreases rather than increases with an increase in outer-tank compressive force at a given torque input. This condition might indicate that nonlinearity is a property of a particular weight condition or frequency. It was observed that the two response peaks tended to coalesce as the outer-tank compressive load was increased.

Comparison with Full-Scale Results

Results of a torsional ground vibration survey of a full-scale Saturn SA-1 vehicle conducted at the Marshall Space Flight Center are presented in reference 4. The frequencies obtained from this survey are plotted in figure 12, where they have been multiplied by the scale factor of 5, for comparison with model results. The scale factor of 5 was determined from the following relationships:

Length:

$$\frac{L_M}{L_F} = \frac{1}{5}$$

Material properties:

$$\frac{G_M}{G_F} = \frac{\rho_M}{\rho_F} = 1$$

Mass:

$$\frac{m_M}{m_F} = \frac{\rho_M}{\rho_F}\left(\frac{L_M}{L_F}\right)^3 = \frac{1}{5^3}$$

Rotational mass moment of inertia:

$$\frac{I_M}{I_F} = \frac{m_M}{m_F}\left(\frac{L_M}{L_F}\right)^2 = \frac{1}{5^5}$$

Torsional stiffness constant:

$$\frac{J_M}{J_F} = \left(\frac{L_M}{L_F}\right)^4 = \frac{1}{5^4}$$

Torsional frequency:

$$\frac{f_M}{f_F} = \left[\frac{(GJ)_M}{(GJ)_F}\,\frac{I_F L_F}{I_M L_M}\right]^{1/2} = 5$$

Figure 12 shows fairly good agreement between the full-scale and model first torsion and first cluster frequencies. The full-scale rigid-body frequency was approximately 100 percent higher than the model rigid-body frequency. The full-scale first torsion frequency was higher than the model first torsion frequency and this difference increased with an increase in booster water level. At the booster full condition, the full-scale frequency was 10 percent higher than the model frequency as compared with 1.5 percent at the empty condition. This difference may be attributed to a difference in the torque level used between the two model tests, and/or may be a function of the outer lox-tank compressive load.

Model and full-scale damping factors are compared in table IV. This figure shows that the model and full-scale damping values are of the same order of magnitude, except for the value of 0.18 given for the full-scale vehicle at the booster empty condition. (No explanation was given in ref. 4 for this high value of damping.)

Comparison with Analytical Results

Calculated fundamental torsional frequencies at three weight conditions are presented in figure 12 (diamond symbol). The calculation was based on a finite-difference method in which the model was considered free-free. The model was subdivided into 30 mass moments of inertia concentrated along the longitudinal axis and interconnected by calculated torsional stiffness factors. The analysis was performed for two cases: (1) the outer-tank inertias distributed along the longitudinal axis of the booster and (2) the outer-tank

inertias brought into the system at the tank ends. Good agreement of frequencies with test results was obtained in the first case where the outer-tank inertias were distributed along the axis. (See fig. 12.) The results from the second case showed poor agreement for the booster-full and maximum-dynamic-pressure configurations, 14.25 cps and 20.25 cps, respectively; but good correlation for the empty configuration, 39.02 cps. It would seem that the outer-tank inertias should be lumped at the tank ends because of their attachments in the booster; however, the model response indicates a node in the booster area that renders much of this inertia ineffectual.

The inertia of the water on the center line of the model in the three stages was neglected. The booster center lox tank was the only structural member considered in calculating the rotational stiffness in the booster tank area.

Since no branches were included in the mathematical model used herein, the outer-tank resonances were not expected to be calculated.

CONCLUDING REMARKS

An investigation of the torsional vibration characteristics of a 1/5-scale model of Saturn SA-1 supported by an eight-cable suspension system has been performed at the Langley Research Center and the results are reported herein. The results consist of the experimental resonant frequencies, the associated mode shapes, and the damping of the 1/5-scale model obtained at three flight conditions of the full-scale vehicle over a frequency range of 20 cps to 70 cps.

These results show the unusual response characteristics of the Saturn model associated with the clustered construction of the booster stage. They show how the elasticity of the spider beam altered the phasing of the outer tank with respect to the center line of the model. Many of the response characteristics of the model are defined by the independent bending of the outer tanks, engines, and outrigger supporting members. The results also show the importance of properly scaling engine support structures in order to determine adequately the model response characteristics.

A large change in the rotational mass moment of inertia is obtained by varying the booster water level. The first torsion mode was increased about 53 percent by varying the booster water level from a full to an empty weight condition.

The first torsion mode and a variety of booster modes were the only modes observed within the frequency range of 20 cps to 70 cps. Comparisons with full-scale results show fairly good agreement for the first torsion and first cluster frequencies. A simplified mathematical model study based on a finite difference method gave good results for the first torsion mode only.

Langley Research Center,
National Aeronautics and Space Administration,
Langley Station, Hampton, Va., December 11, 1964.

REFERENCES

1. Mixson, John S.; Catherine, John J.; and Arman, Ali: Investigation of the Lateral Vibration Characteristics of a 1/5-Scale Model of Saturn SA-1. NASA TN D-1593, 1963.

2. Mixson, John S.; and Catherine, John J.: Experimental Lateral Vibration Characteristics of a 1/5-Scale Model of Saturn SA-1 With an Eight-Cable Suspension System. NASA TN D-2214, 1964.

3. Mixson, John S.; and Catherine, John J.: Comparison of Experimental Vibration Characteristics Obtained From a 1/5-Scale Model and From a Full-Scale Saturn SA-1. NASA TN D-2215, 1964.

4. Propulsion and Vehicle Engineering Division: Experimental Vibration Program on a Full Scale Saturn Space Vehicle. Appendix B of Saturn Quarterly Progress Report. MPR-SAT-62-3, NASA George C. Marshall Space Flight Center, Jan.-Mar. 1962.

TABLE I.- ENGINE FREQUENCIES

Engine	Tangential frequency, cps
Outboard	
2	32.1
4	29.6
6	34.9
8	35.0
Inboard	
1	50.0
3	85.7
5	52.0
7	80.0

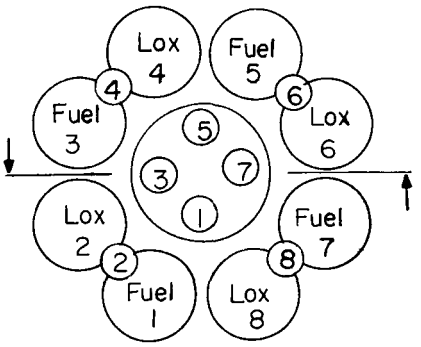

TABLE II.- EXPERIMENTAL ROTATIONAL MOMENT OF INERTIA

	Moment of inertia about longitudinal axis, in-lb-sec^2
First stage	430
Second stage	160.5
Third stage (includes nose cone)	21.3

TABLE III.- TORSIONAL FREQUENCIES AND ASSOCIATED DAMPING

Mode	Booster empty; spring suspension				Booster 48-percent full				Booster full	
	Engines not braced		Engines braced		Spring suspension		Rigid-link suspension		Spring suspension	
	Frequency, cps	Damping, g	Frequency, cps	Damping, g	Frequency, cps	Damping, g	Frequency, cps	Damping, g	Frequency, cps	Damping, g
Rigid body	0.775				0.585		0.589		0.545	
First torsion	38.9	0.0276	35.4		30.2	0.0190	30.3	0.0146	25.36	0.0155
First cluster	63.5		62.5	0.0249	56.2		57.2		28.2	.0342
Coupled bending torsion					50.2		50.4			
Outer-tanks second bending									41.6	.0071
Coupled first torsion, outer-tank second bending					63.1		64.0		46.0	
Booster modes					20.8 27.2 45.5		20.9 27.3 45.0		55.4	.0243
Engine modes	29.2 31.2 34.3				29.66					

TABLE IV.- COMPARISON OF FULL-SCALE WITH

1/5-SCALE MODEL DAMPING, g

Mode	Booster full		Booster 48 percent full		Booster empty	
	Model	Full scale	Model	Full scale	Model	Full scale
First torsion	0.016	0.028	0.019	0.016	0.028	0.18
First cluster	.034	.078				

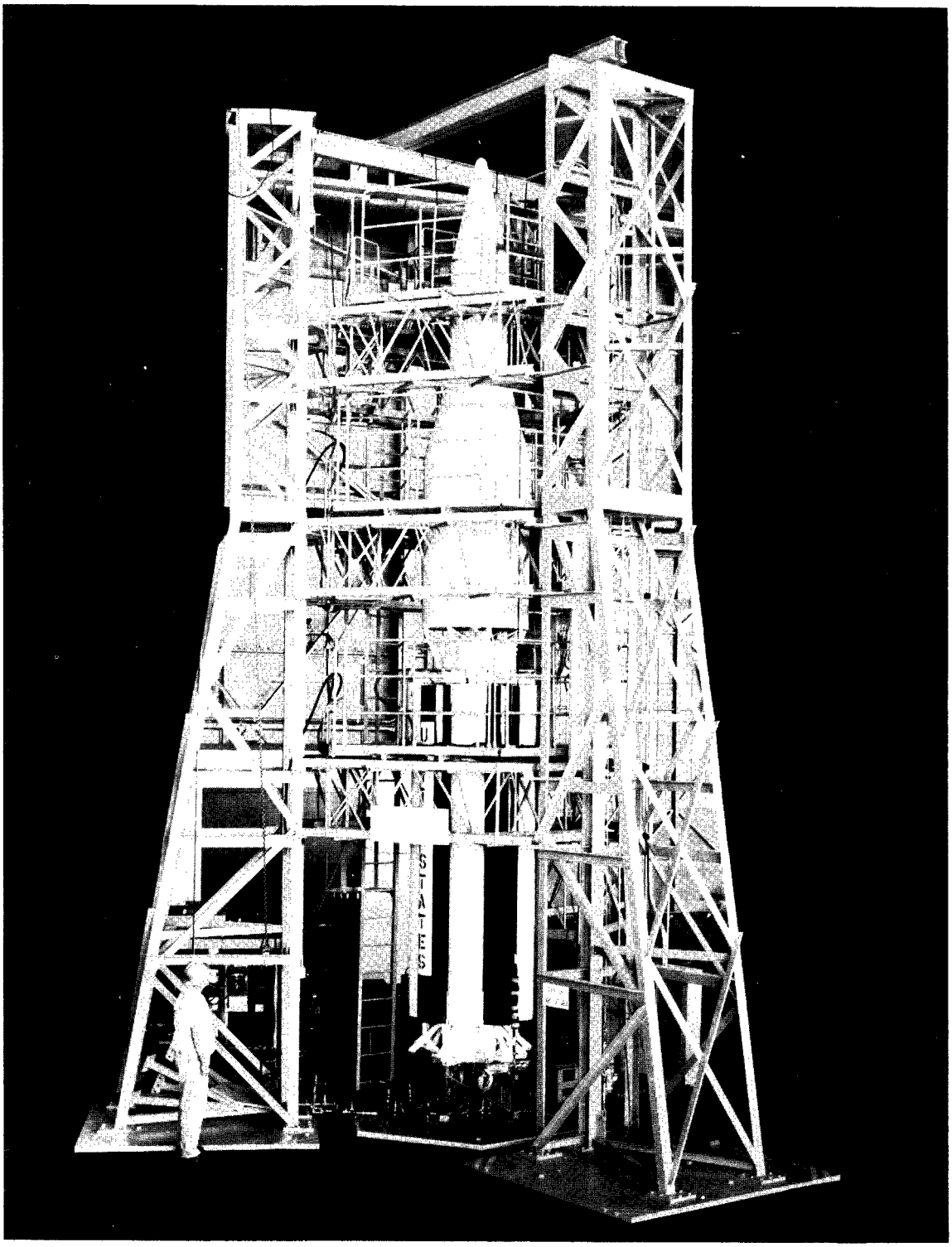

Figure 1.- The 1/5-scale model of Saturn SA-1. L-61-4079

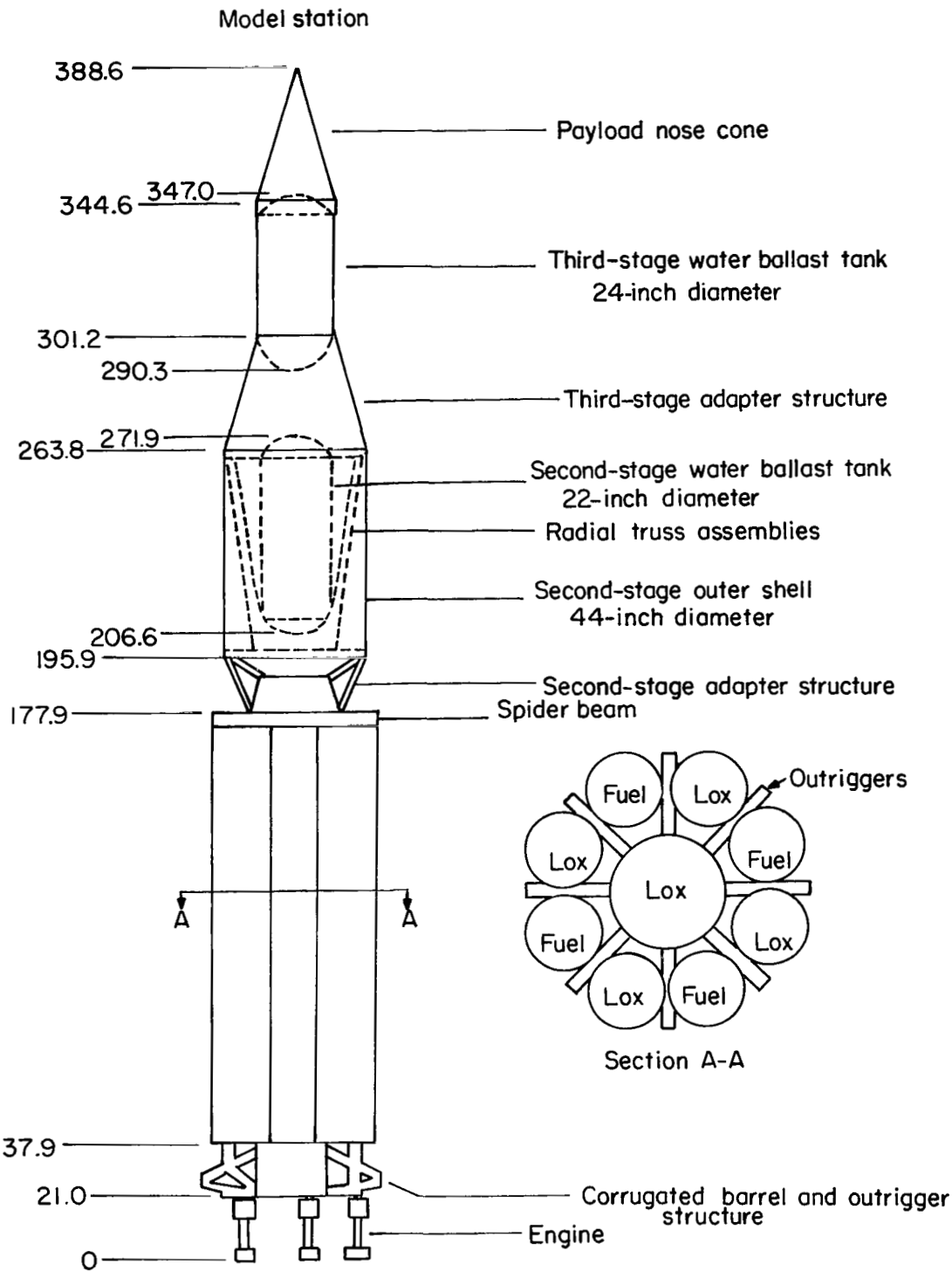

Figure 2.- General configuration and nomenclature of 1/5-scale model of Saturn SA-1. All dimensions are in inches.

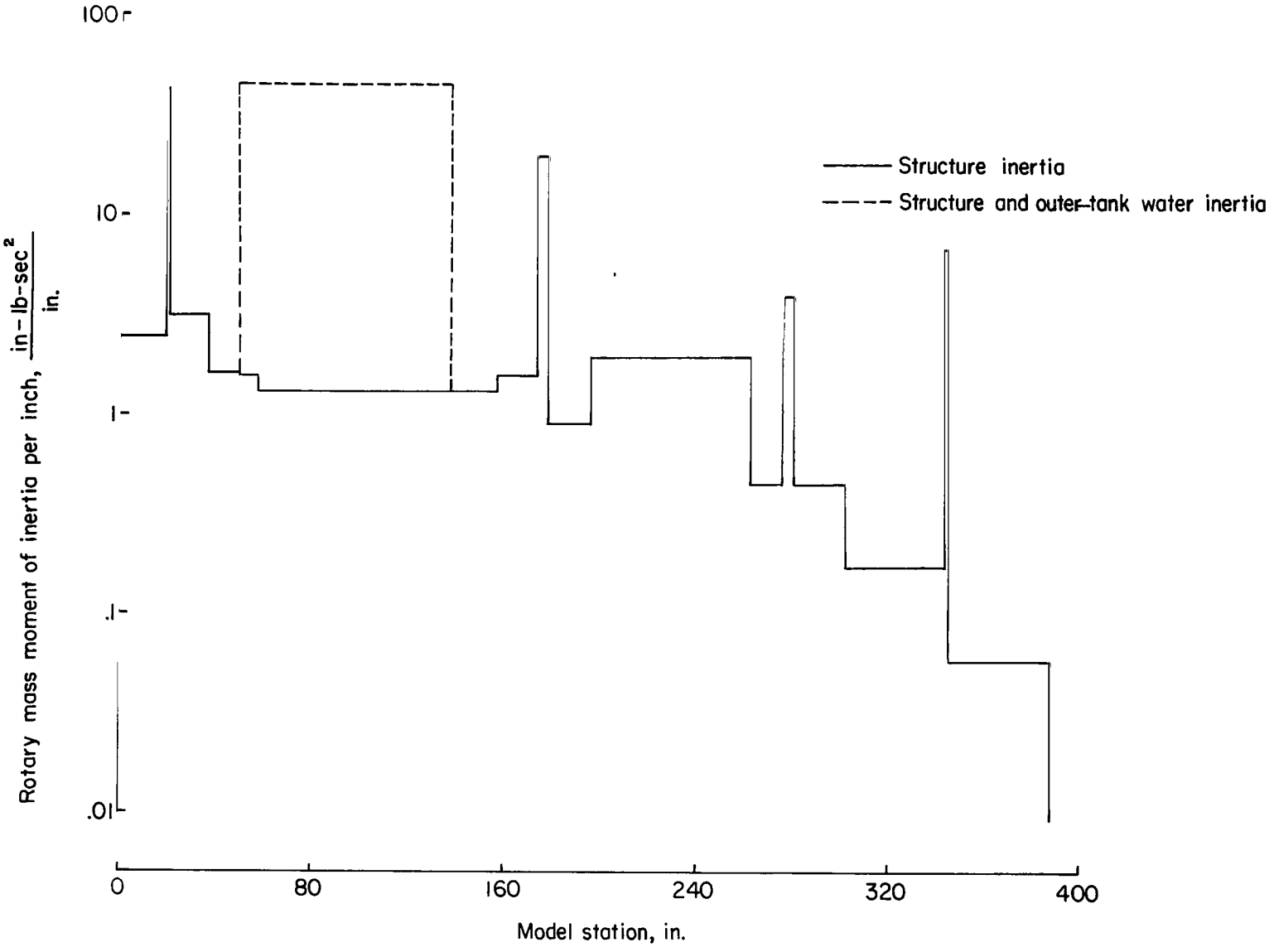

Figure 3.- Distribution of rotary moment of inertia of 1/5-scale Saturn model.

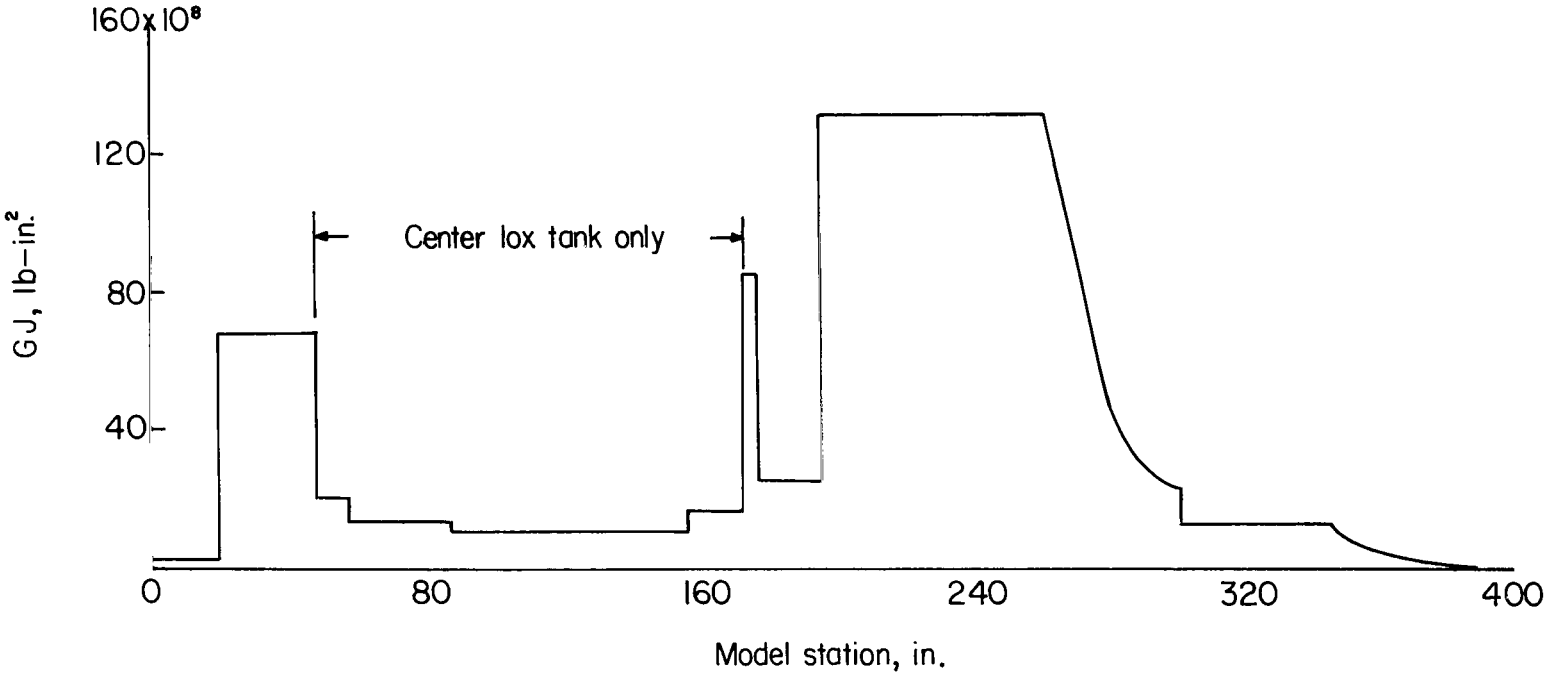

Figure 4.- Torsional stiffness distribution of 1/5-scale Saturn model.

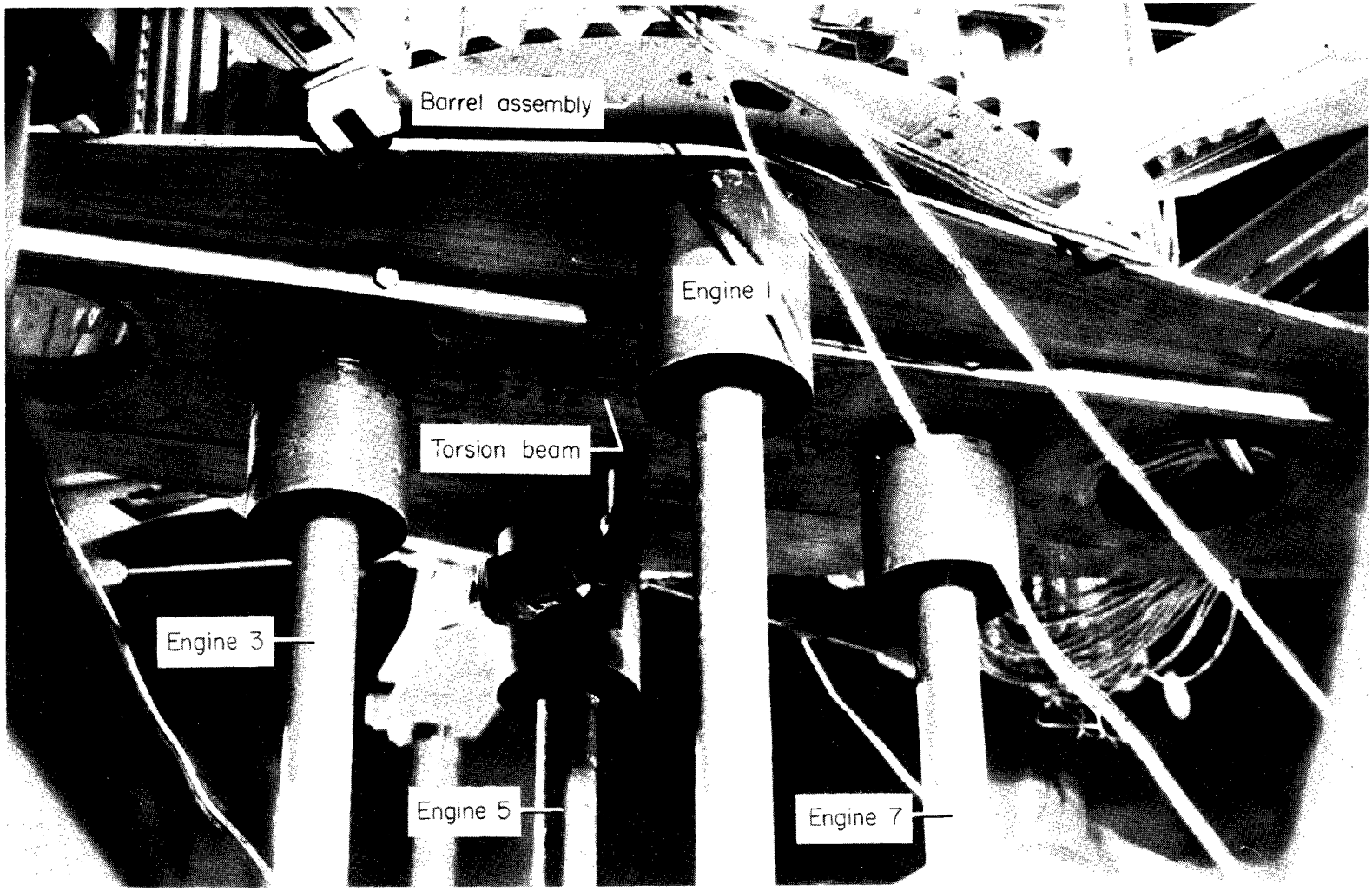

Figure 5.- Torsion beam held in place by mounted inboard engines. L-63-5448.1

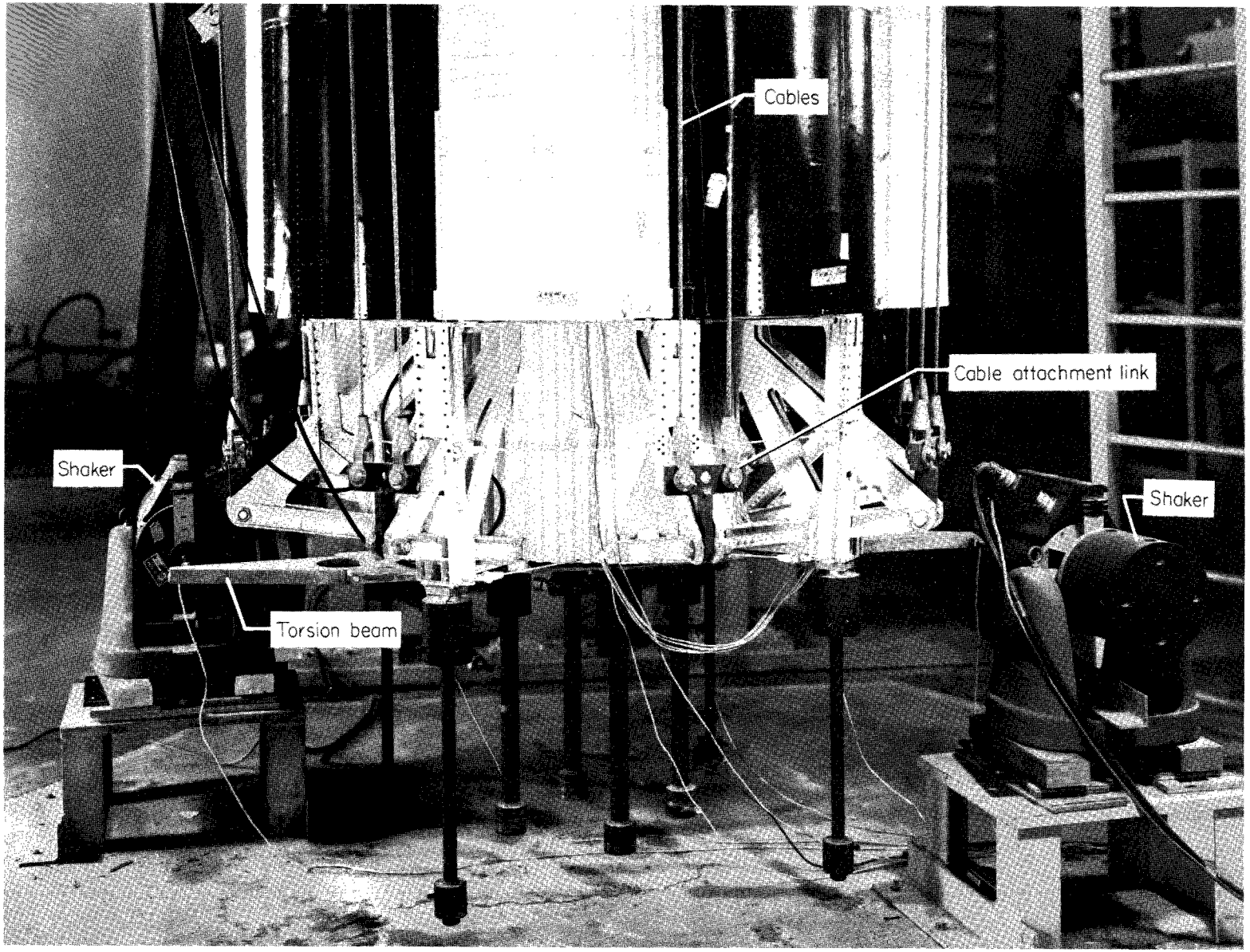

Figure 6.- Eight-cable suspension attachments to outriggers and shaker orientation. L-63-5432.1

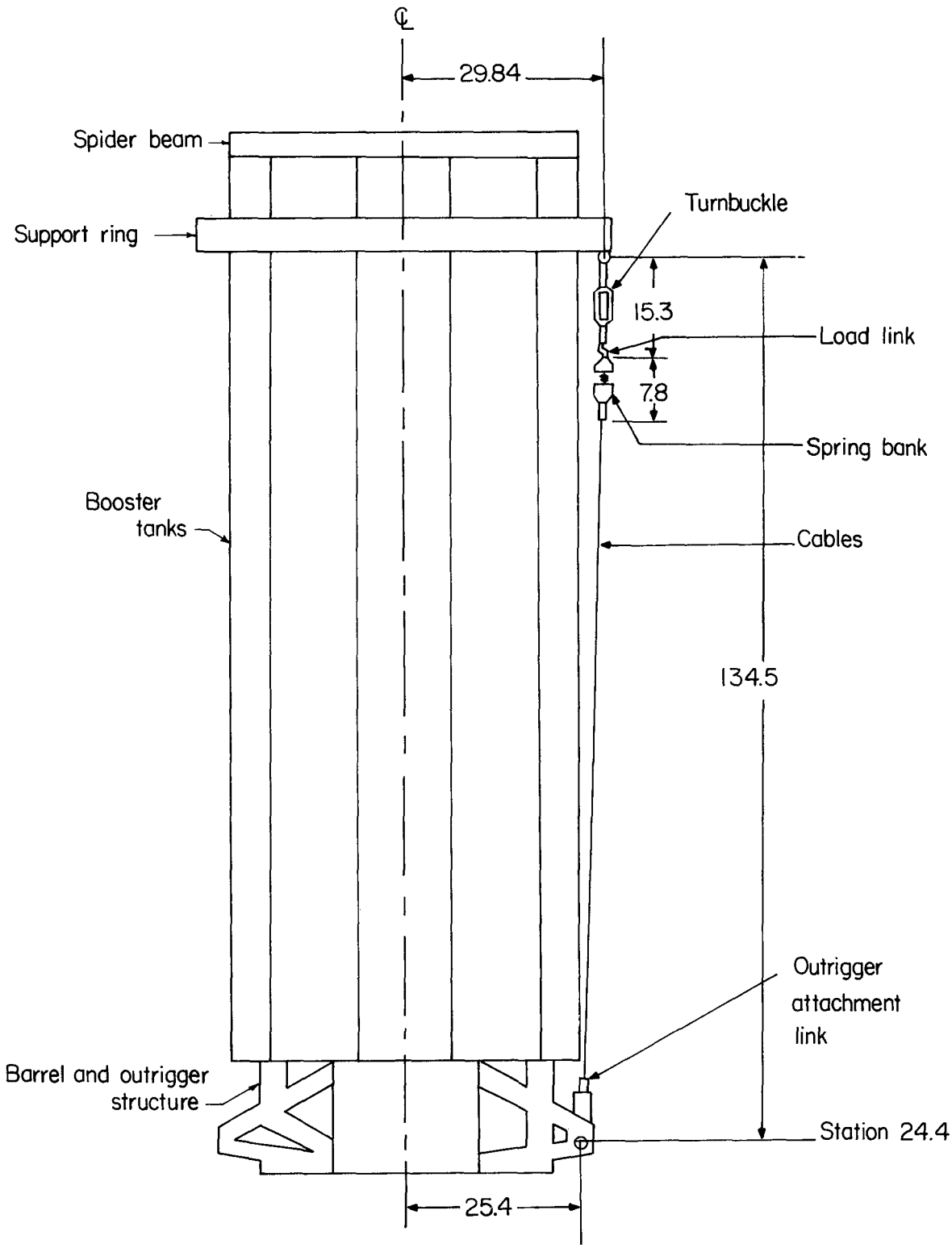

Figure 7.- Eight-cable suspension system. All dimensions are in inches.

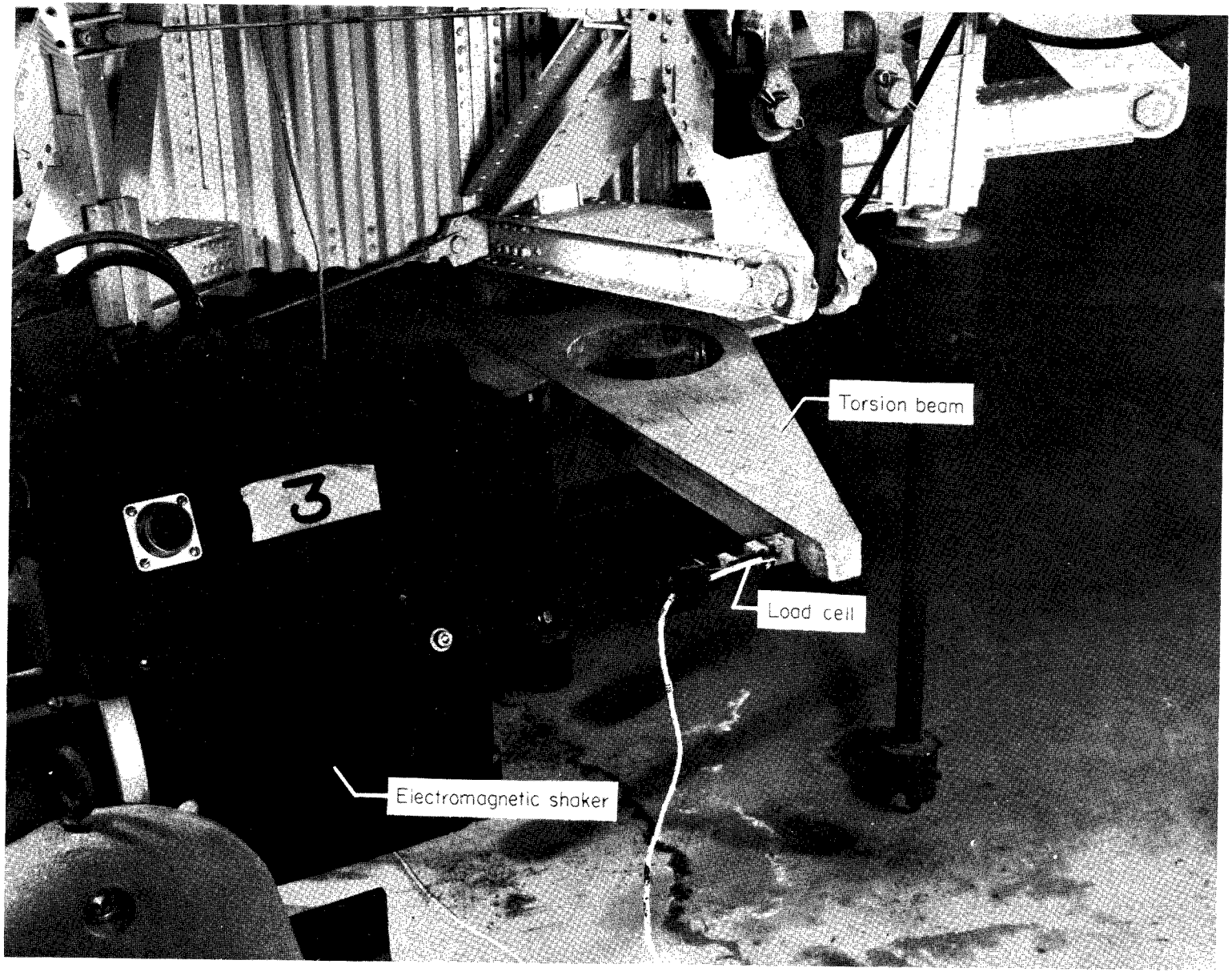

Figure 8.- Typical shaker attachment.

L-63-5431.1

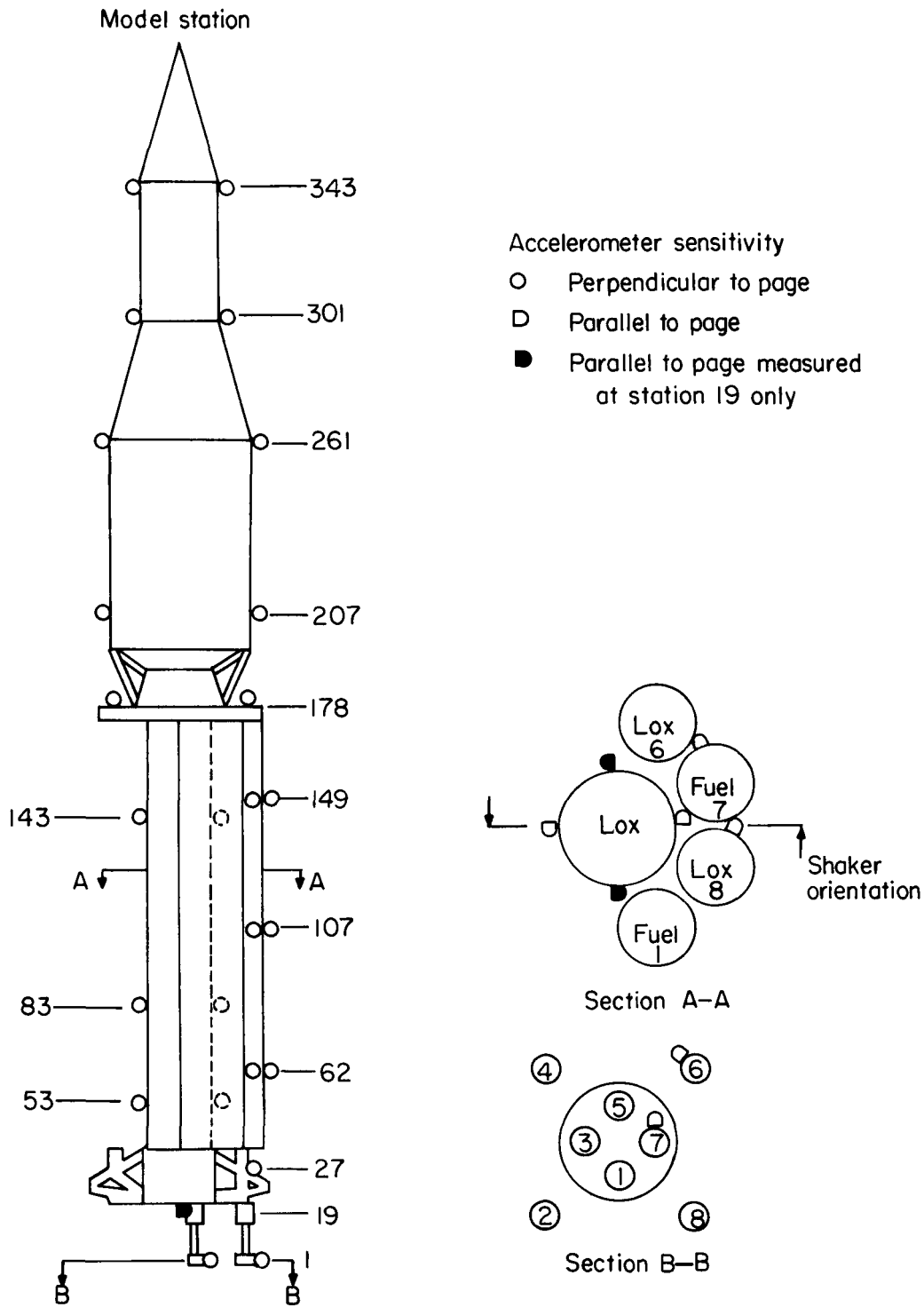

Figure 9.- Fixed accelerometer locations on 1/5-scale Saturn model. All dimensions are in inches.

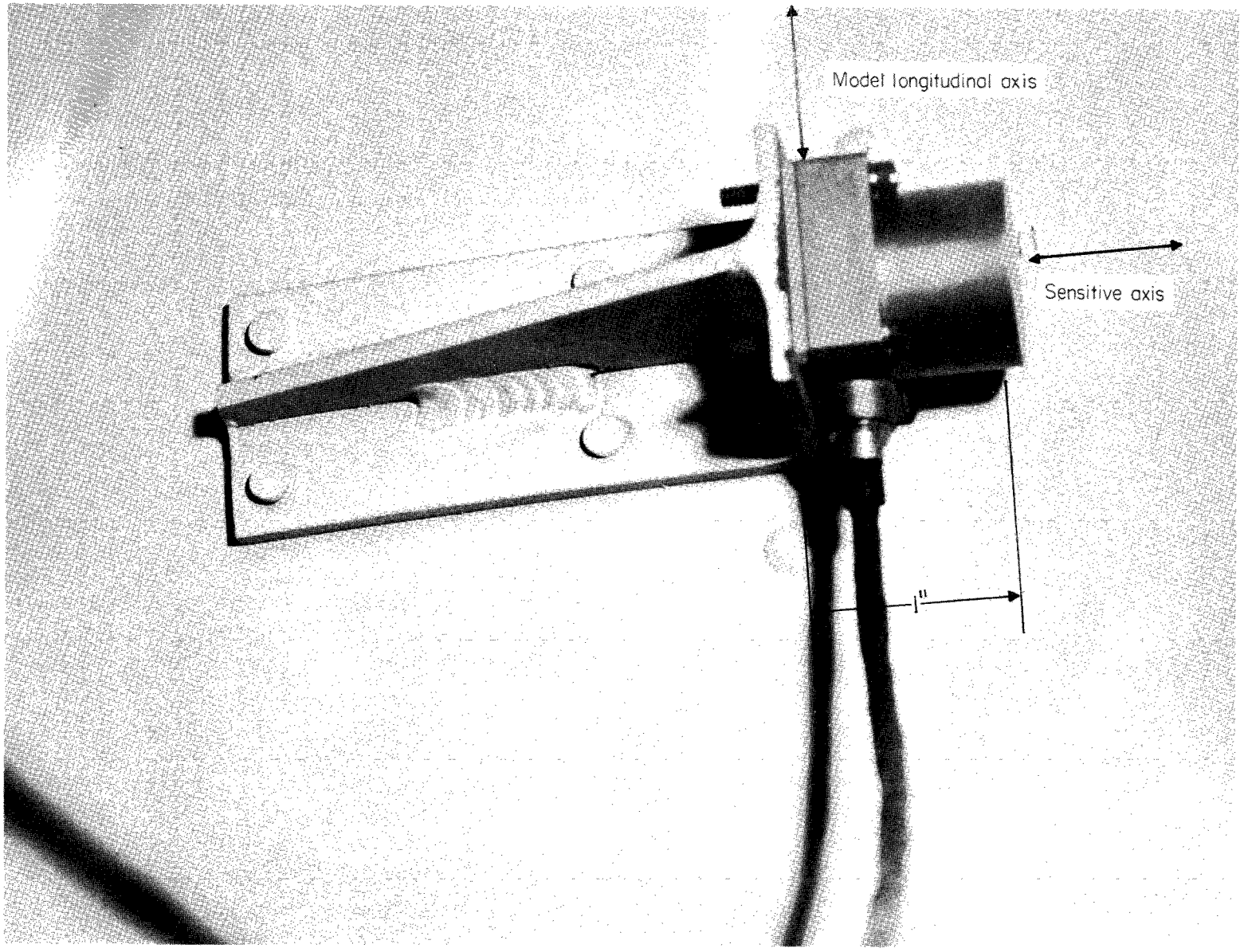

Figure 10.- Typical accelerometer installation for upper stages and center lox tank. L-63-5429.1

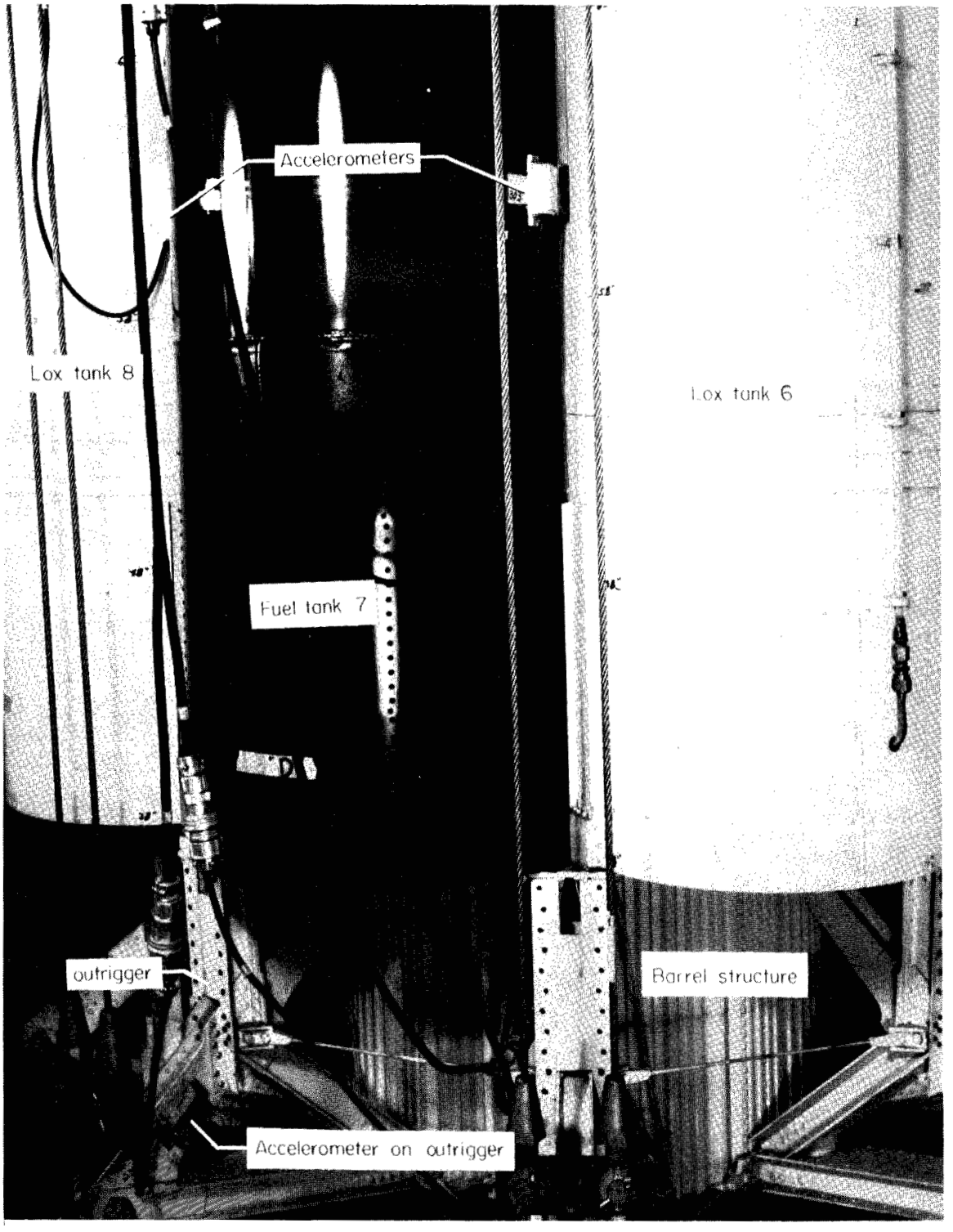

L-63-5433.1

Figure 11.- Booster outer tanks and outriggers showing accelerometer attachments.

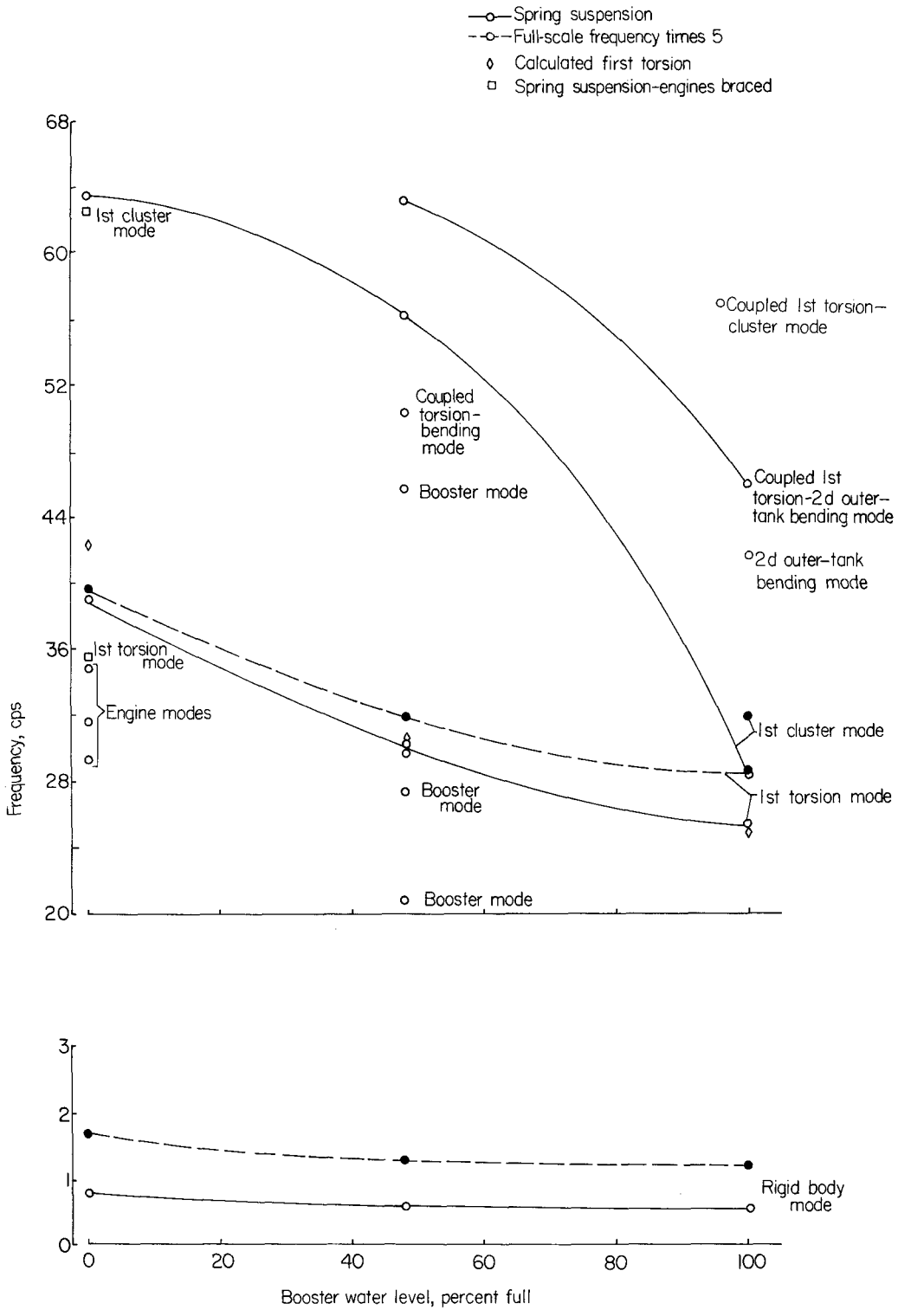

Figure 12.- Variation of resonant frequency with booster water level.

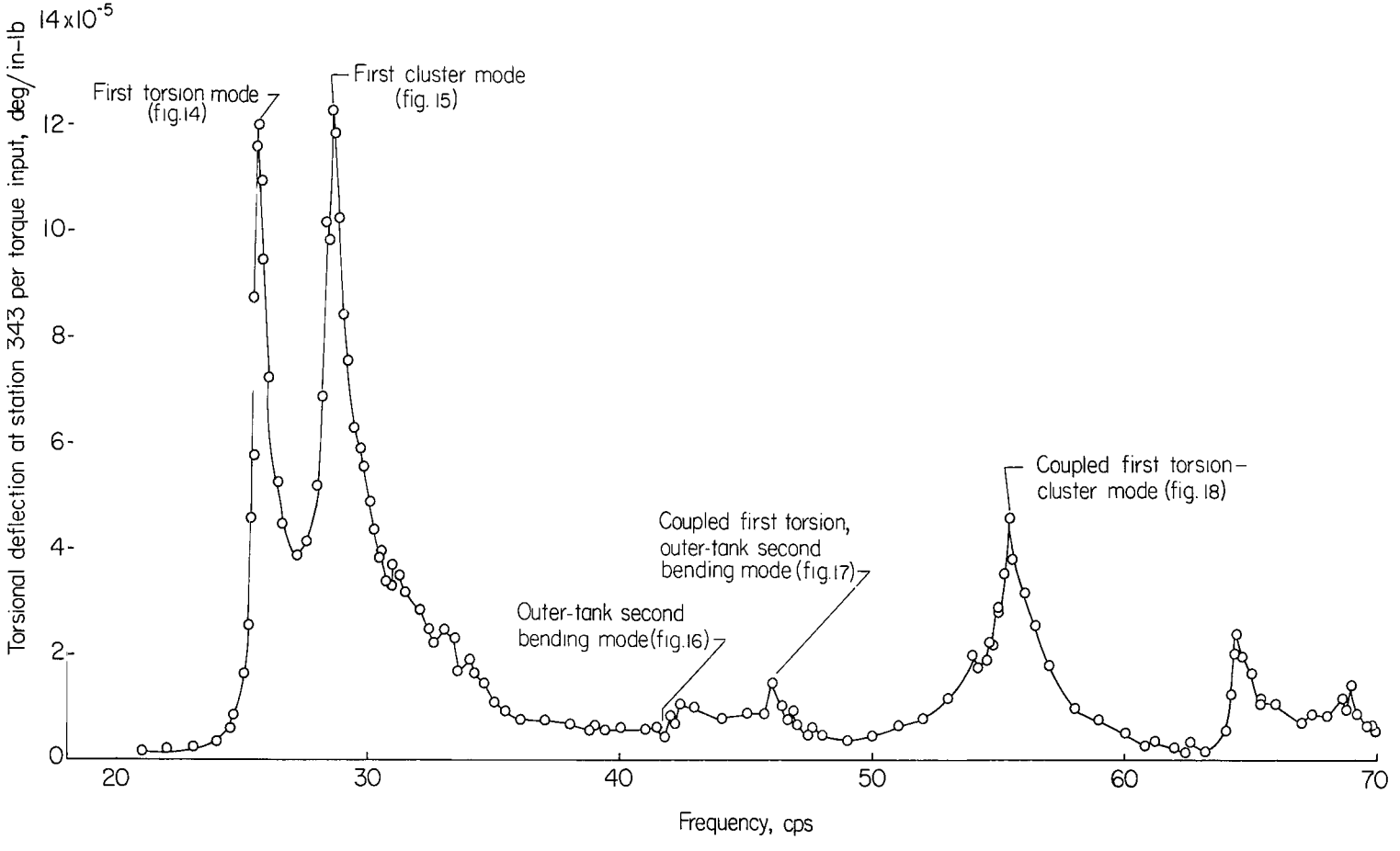

Figure 13.- Frequency response of station 343. Spring suspension; booster full.

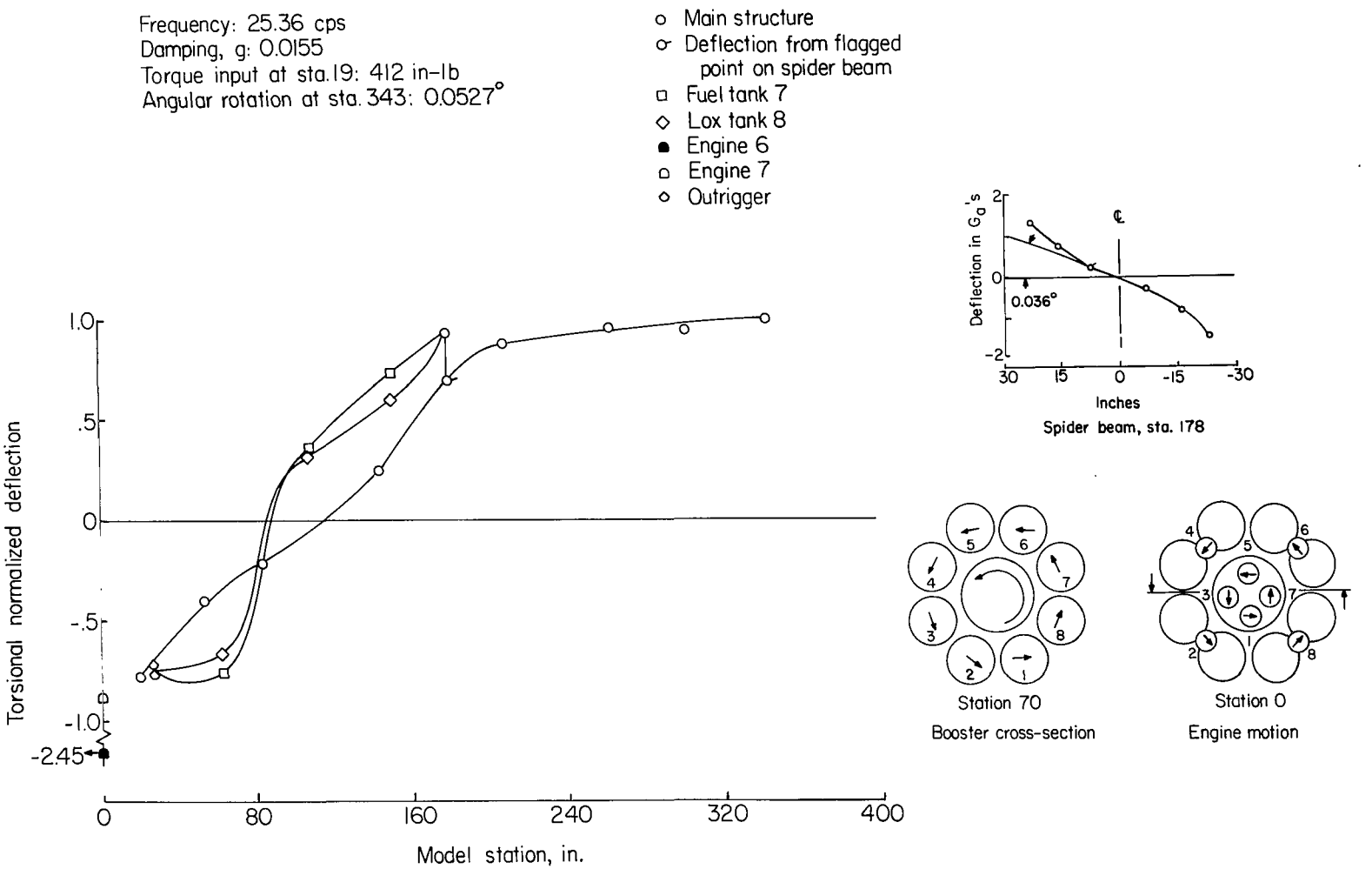

Figure 14.- First torsion mode. Spring suspension; booster full.

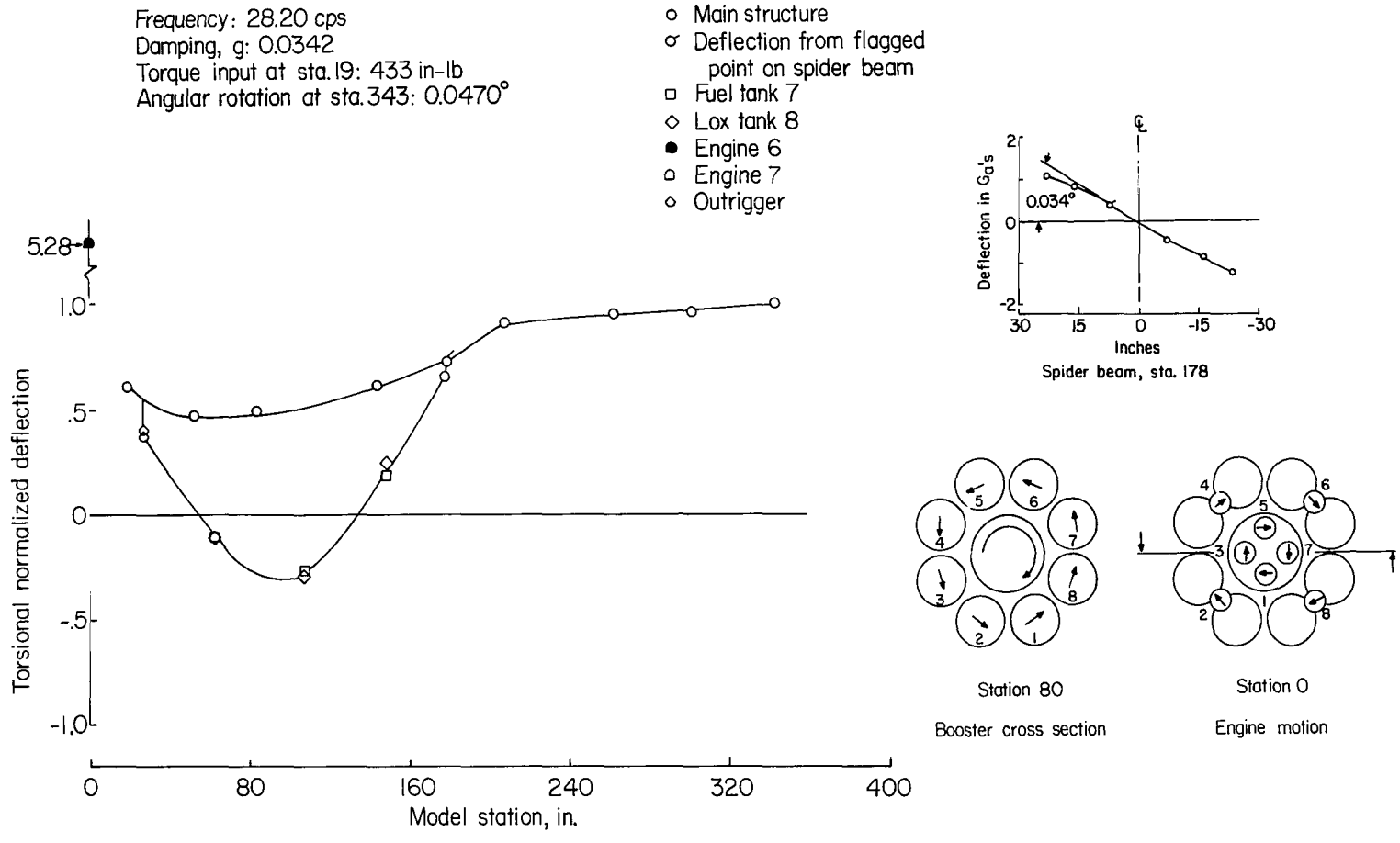

Figure 15.- First cluster mode. Spring suspension; booster full.

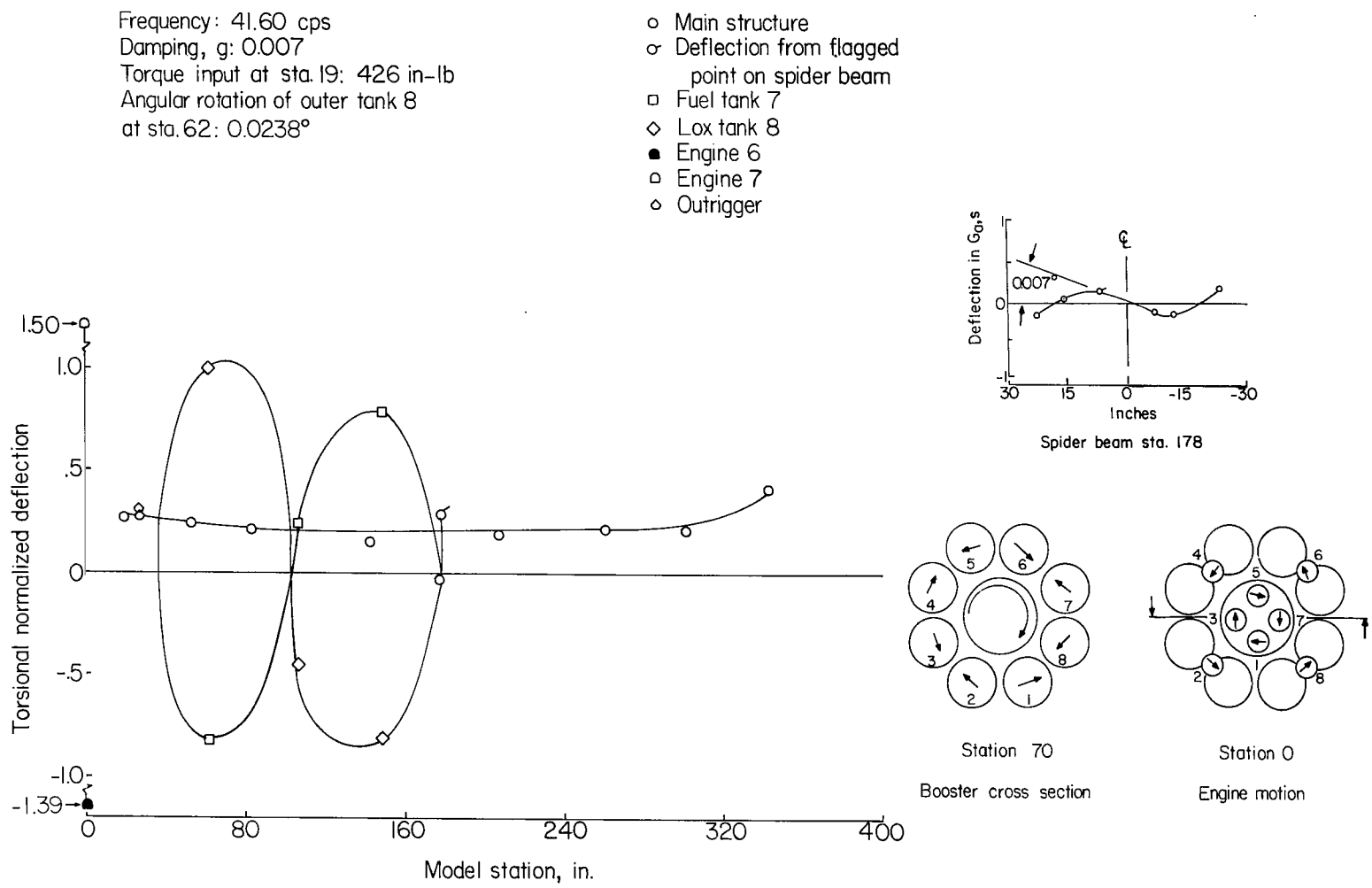

Figure 16.- Outer-tank second bending mode. Spring suspension; booster full.

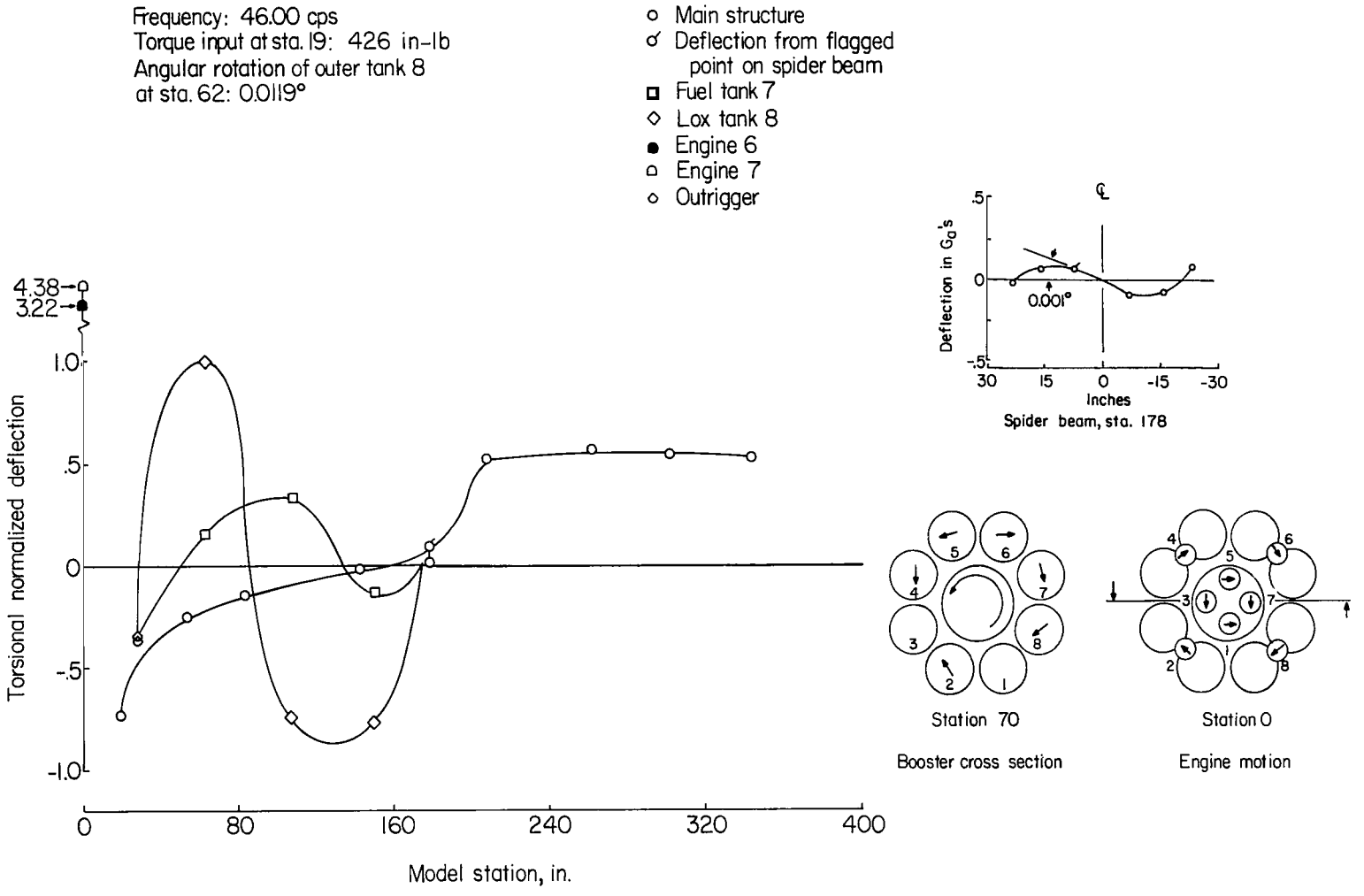

Figure 17.- Coupled first torsion, outer-tank second bending mode. Spring suspension; booster full.

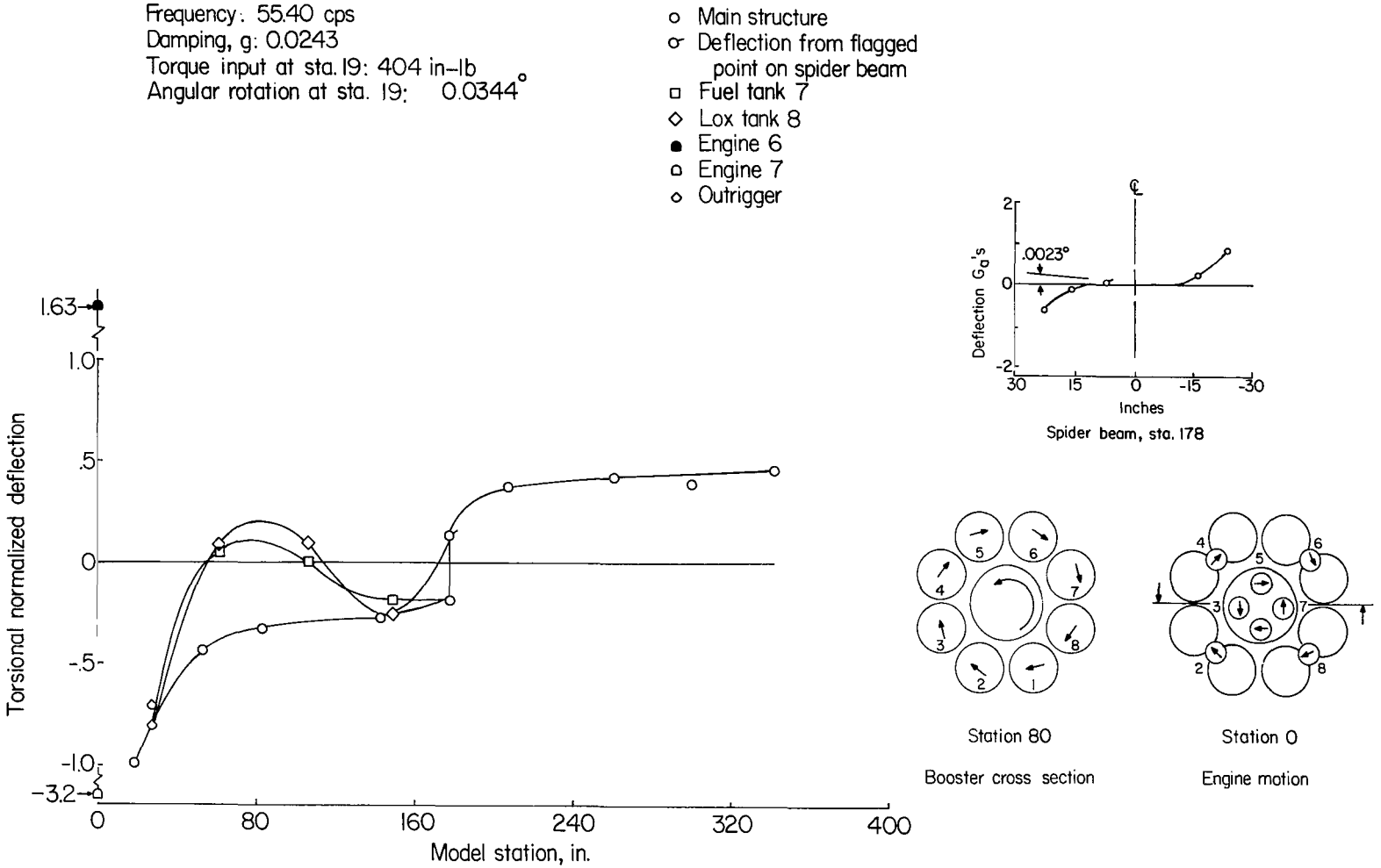

Figure 18.- Coupled first torsion-cluster mode. Spring suspension; booster full.

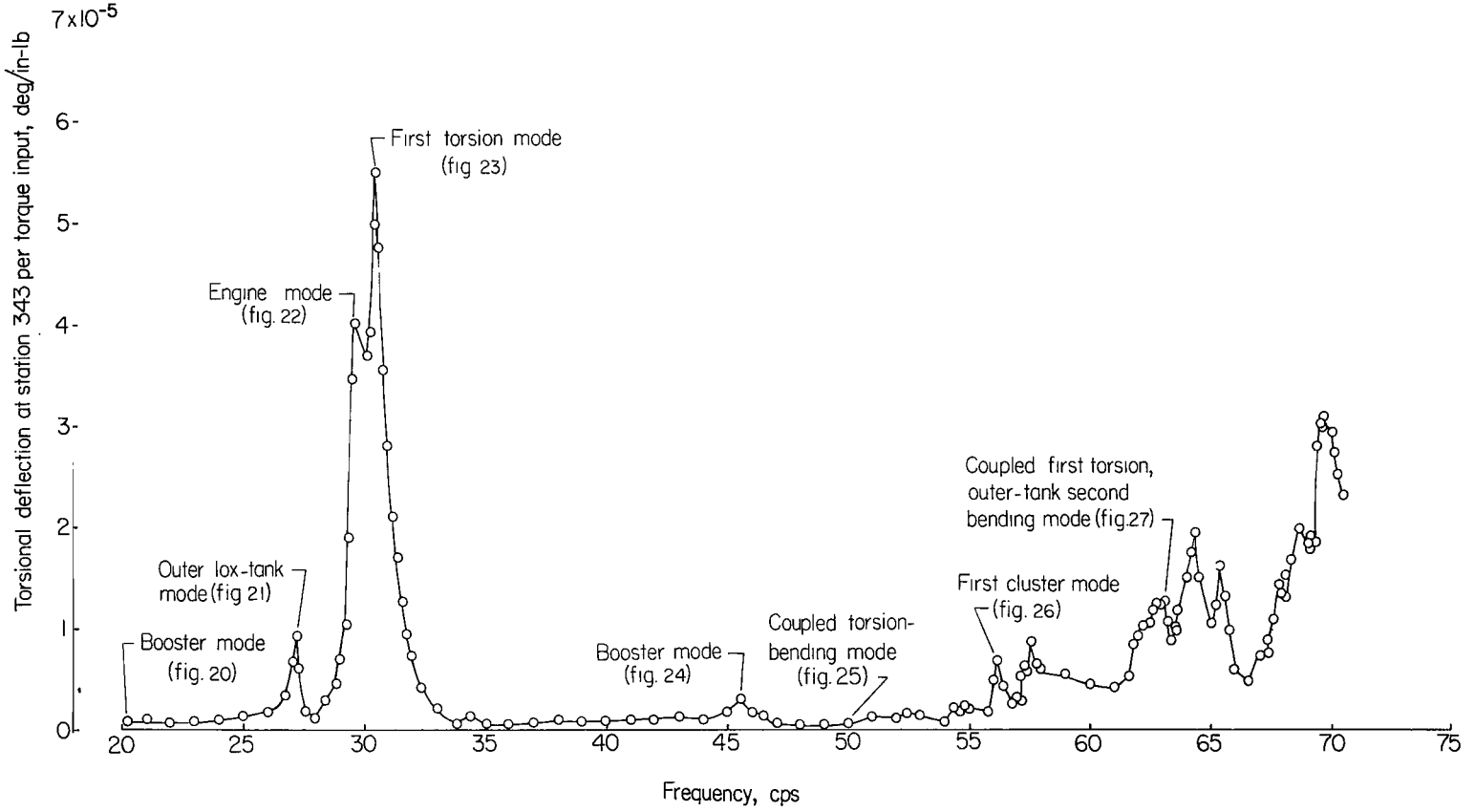

Figure 19.- Frequency response at station 343. Spring suspension; booster 48 percent full.

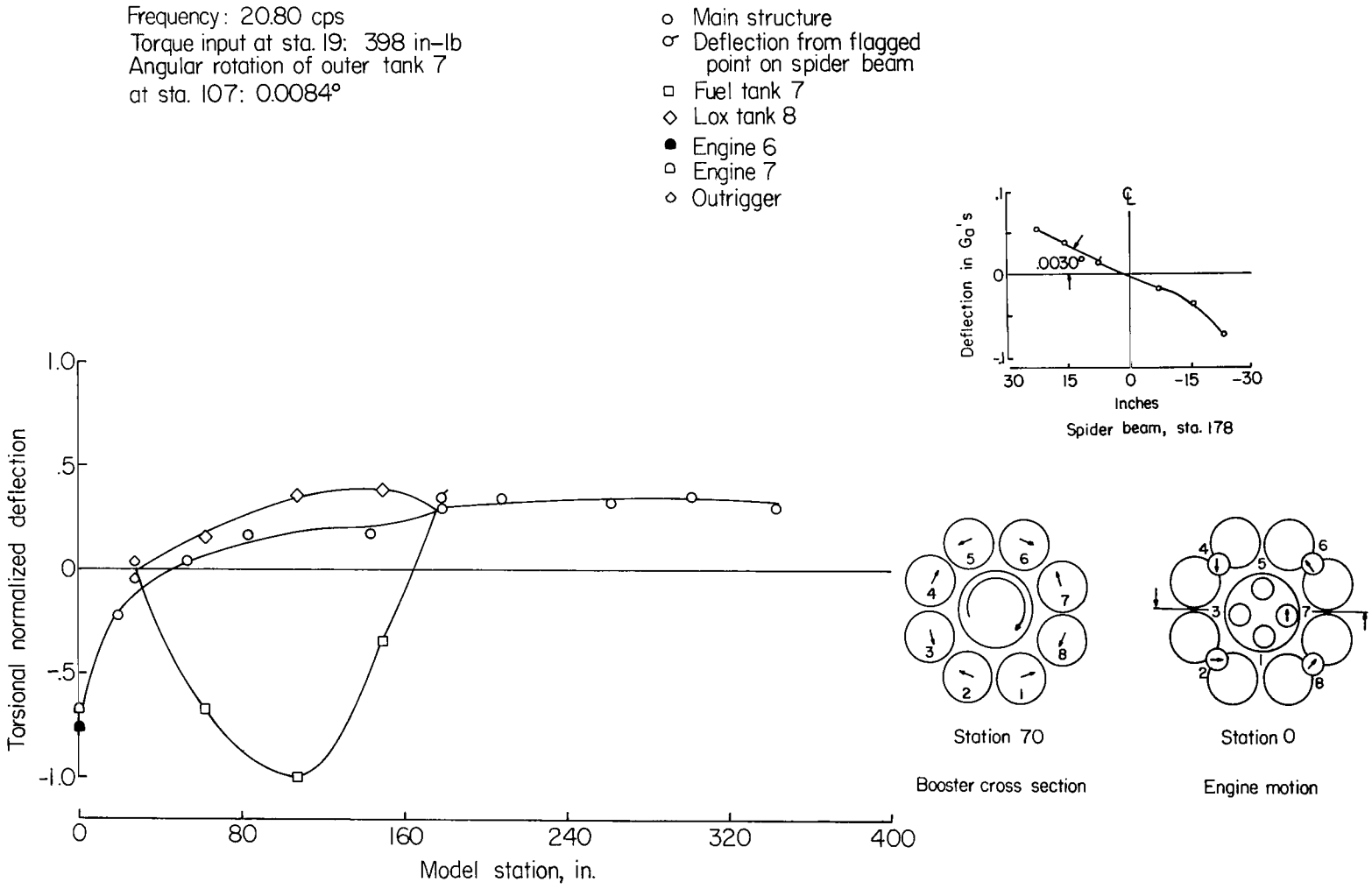

Figure 20.- Booster mode. Spring suspension; booster 48 percent full.

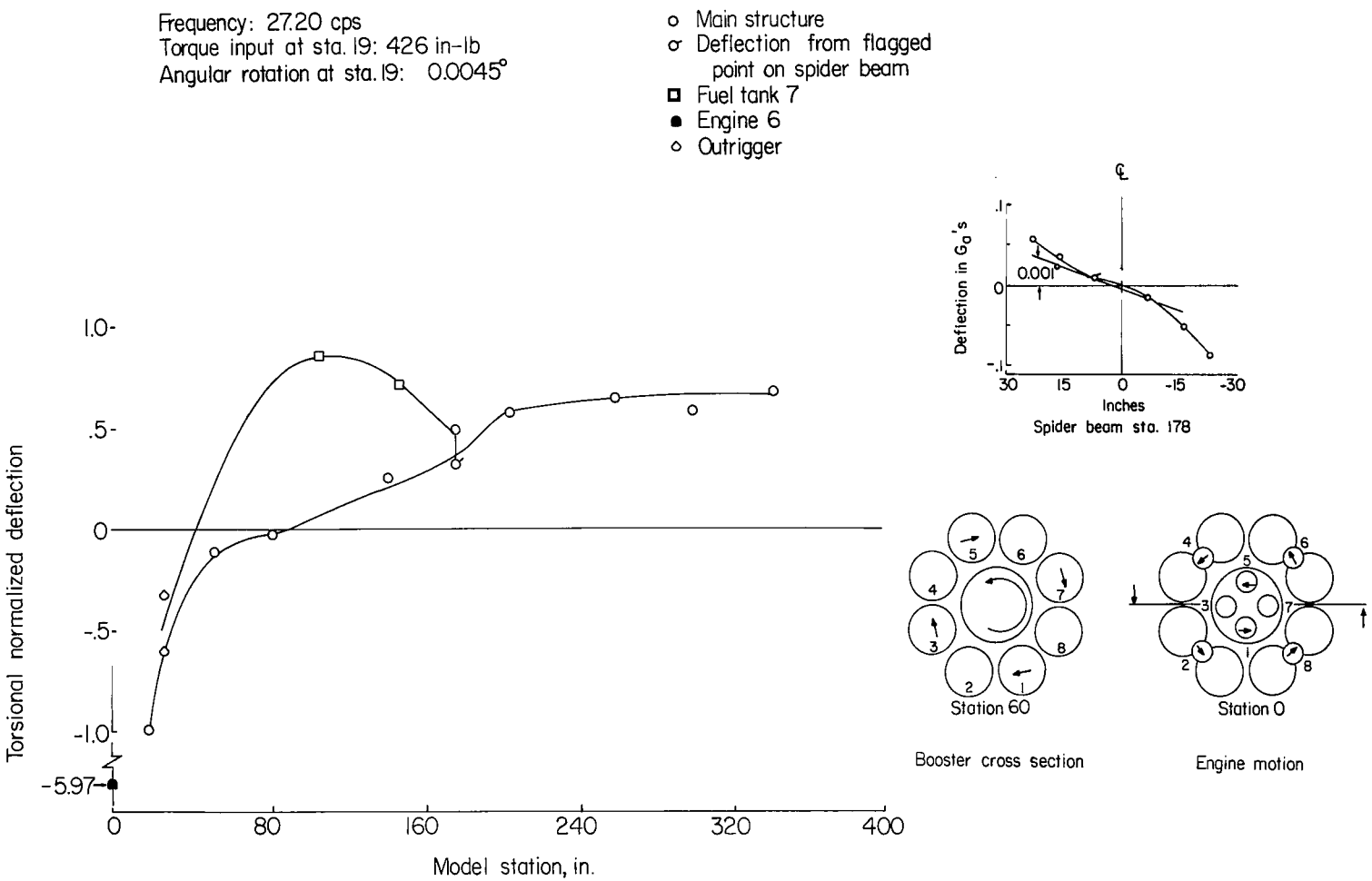

Figure 21.- Outer lox-tank mode. Spring suspension; booster 48 percent full.

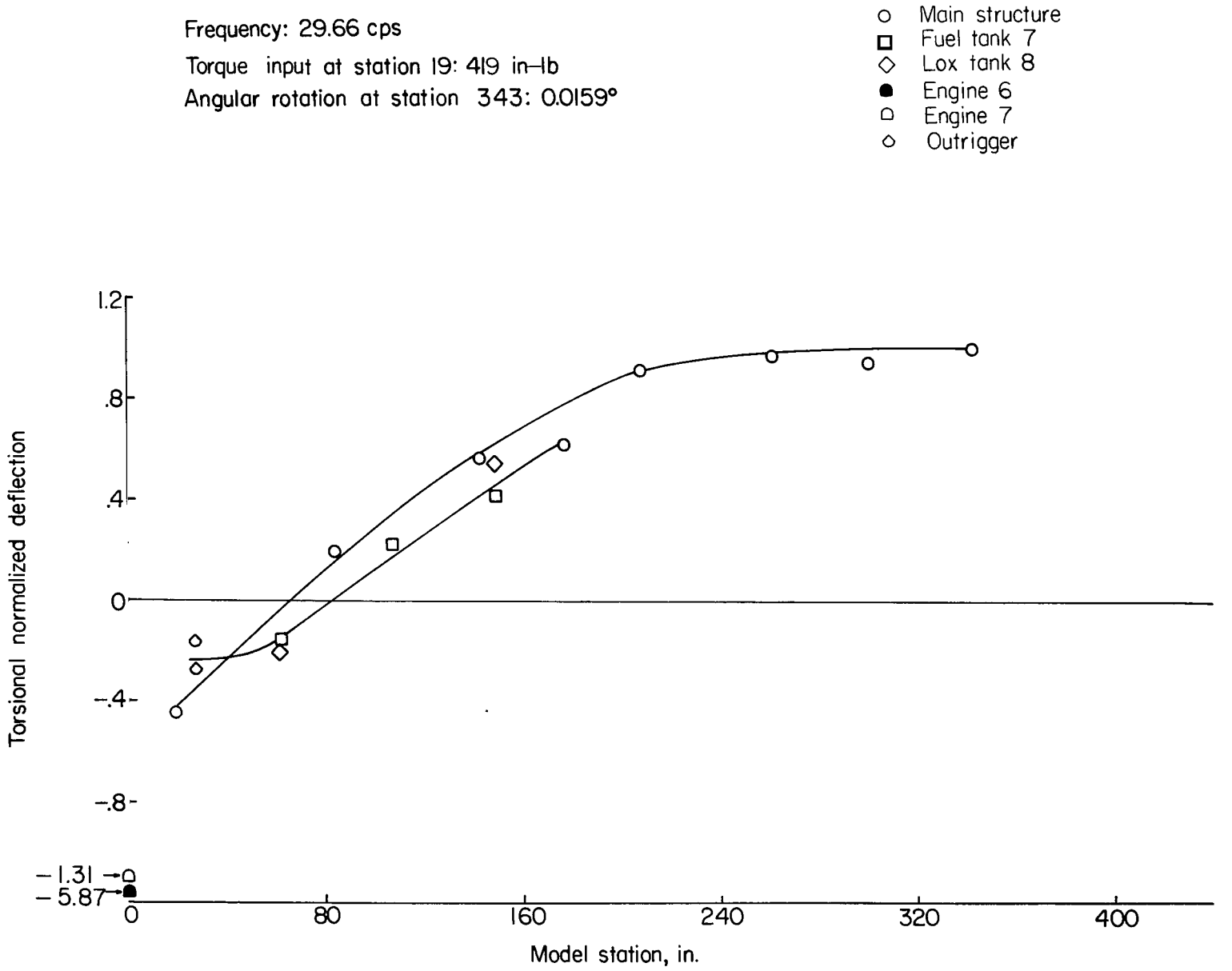

Figure 22.- Engine mode. Spring suspension; booster 48 percent full.

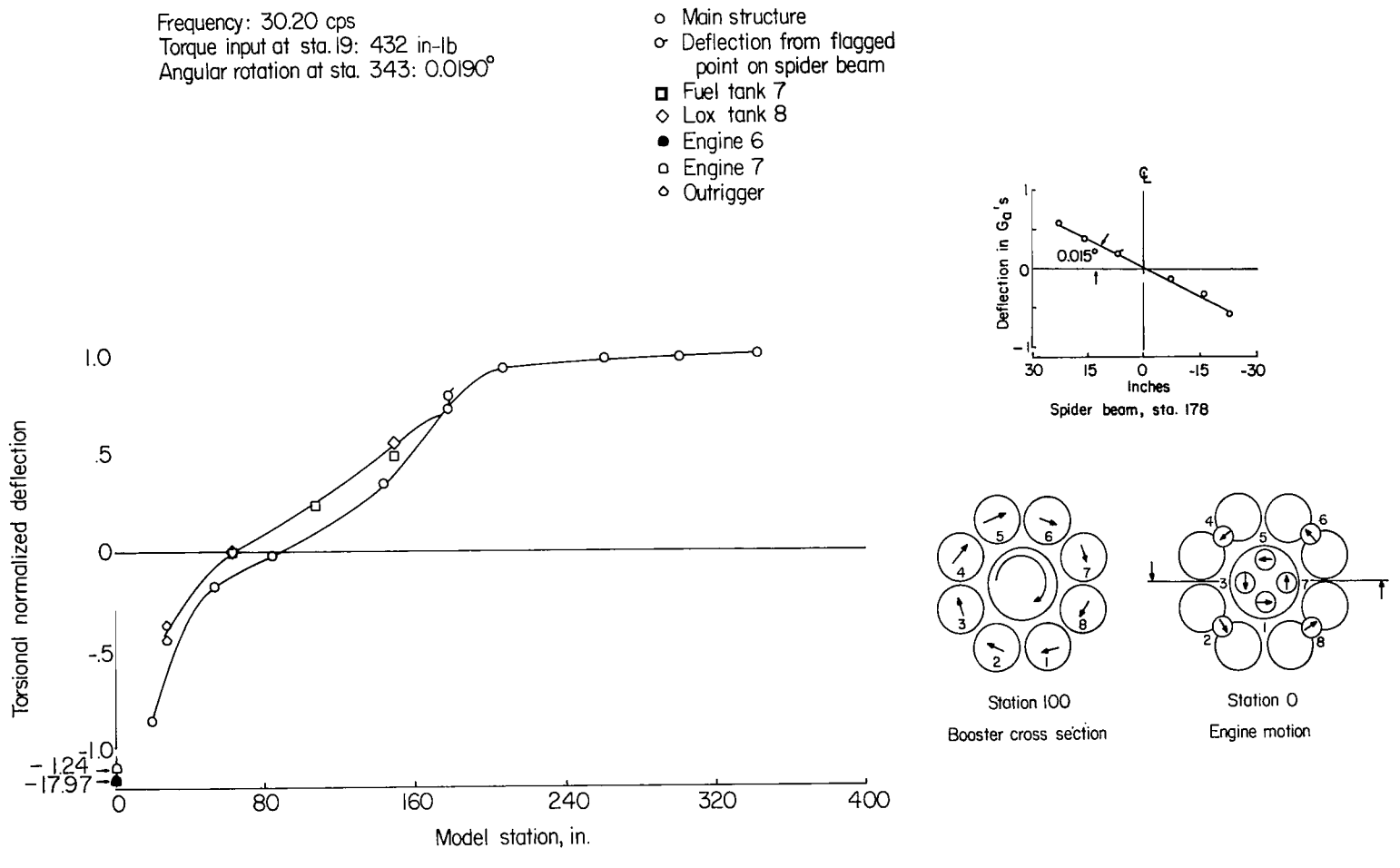

Figure 23.- First torsion mode. Spring suspension; booster 48 percent full.

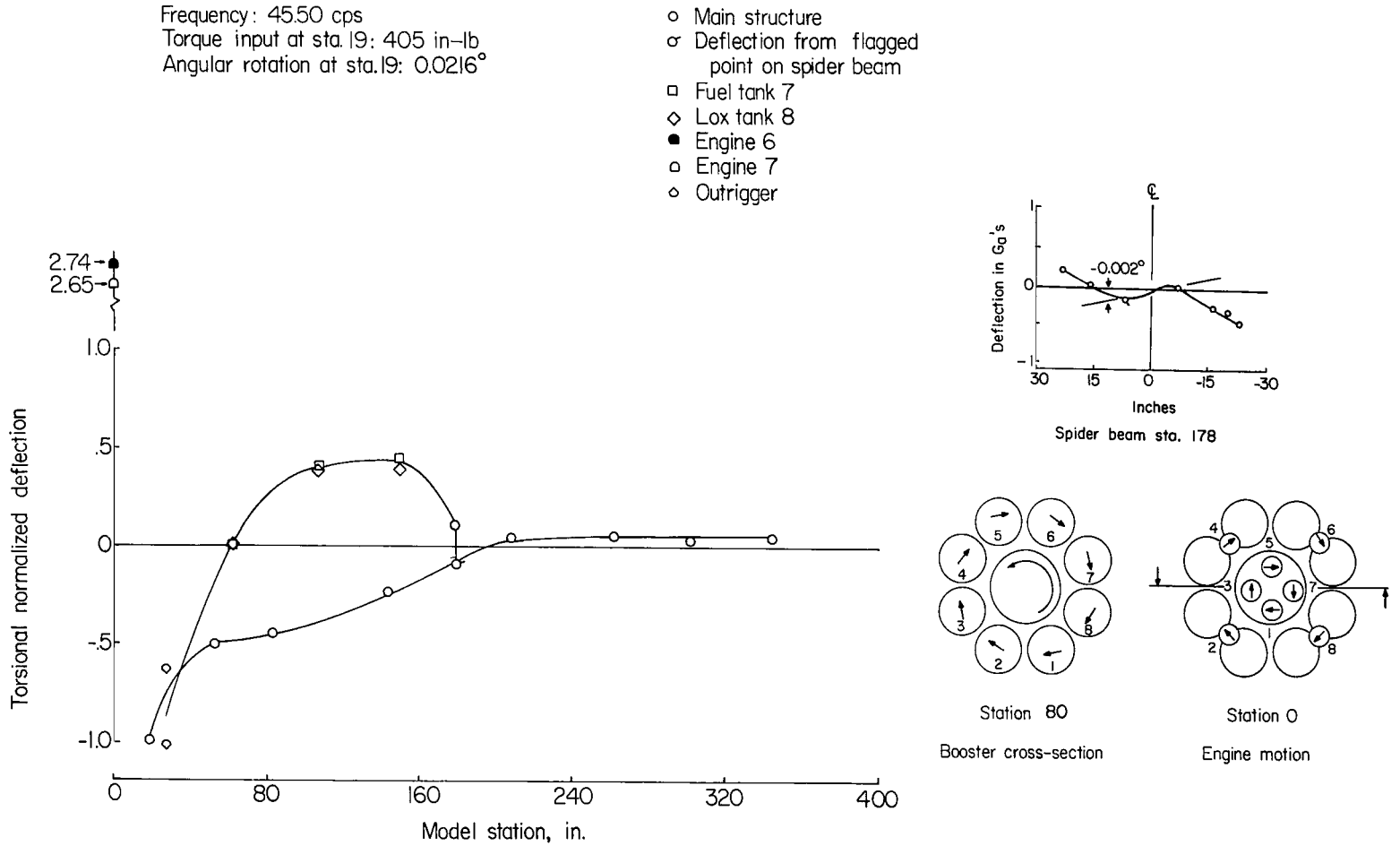

Figure 24.- Booster mode. Spring suspension; booster 48 percent full.

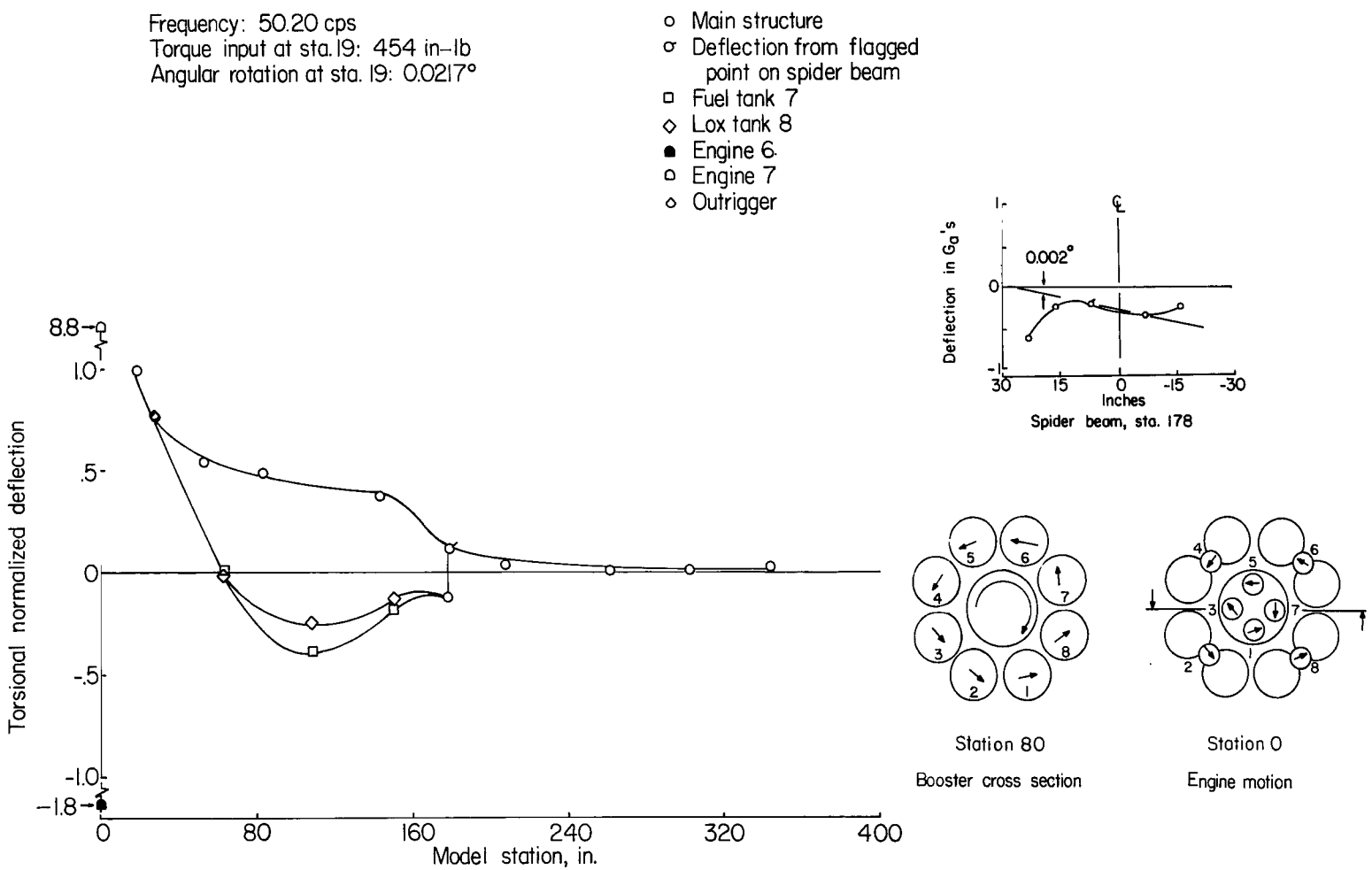

Figure 25.- Coupled torsion-bending mode. Spring suspension; booster 48 percent full.

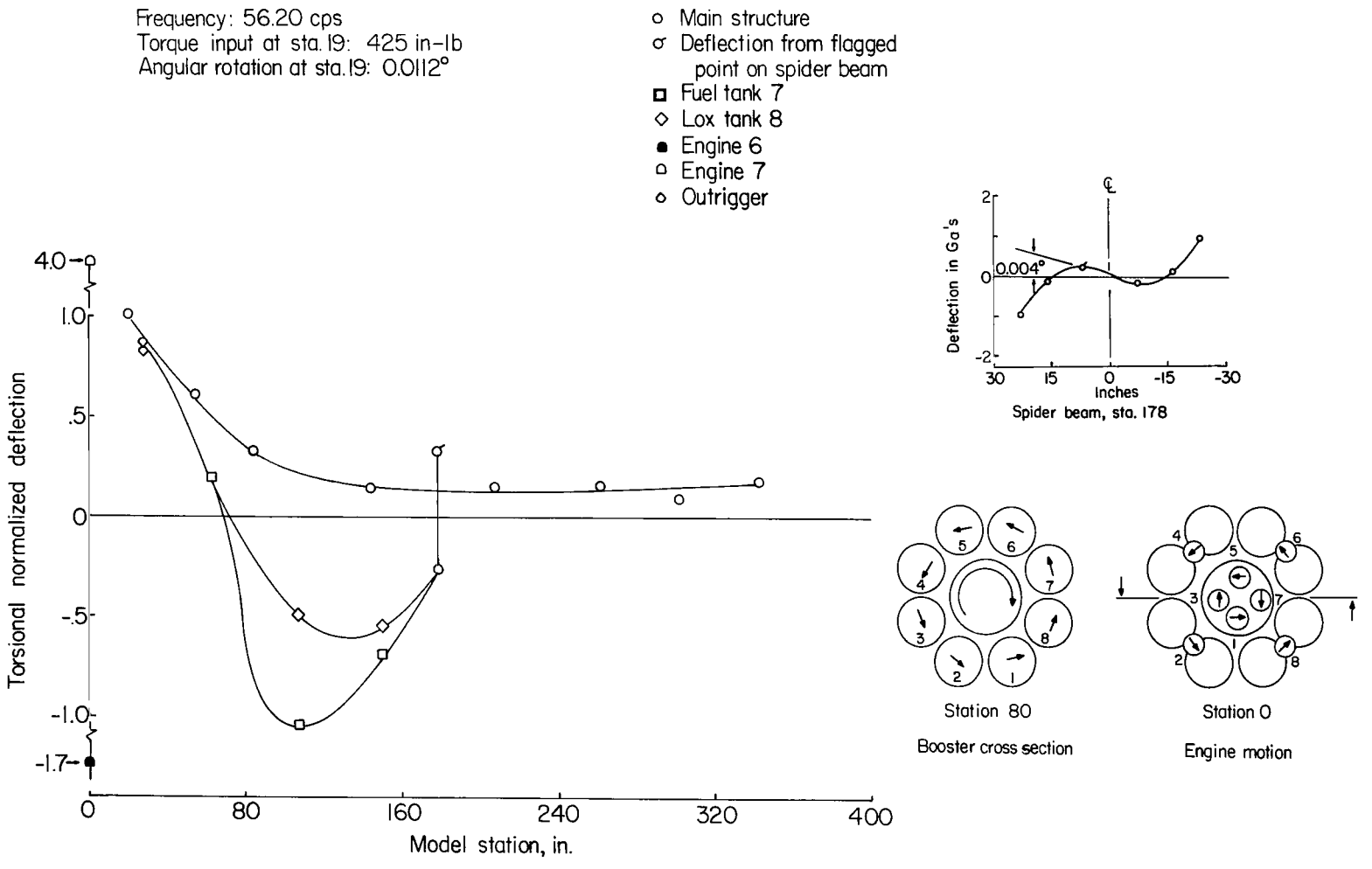

Figure 26.- First cluster mode. Spring suspension; booster 48 percent full.

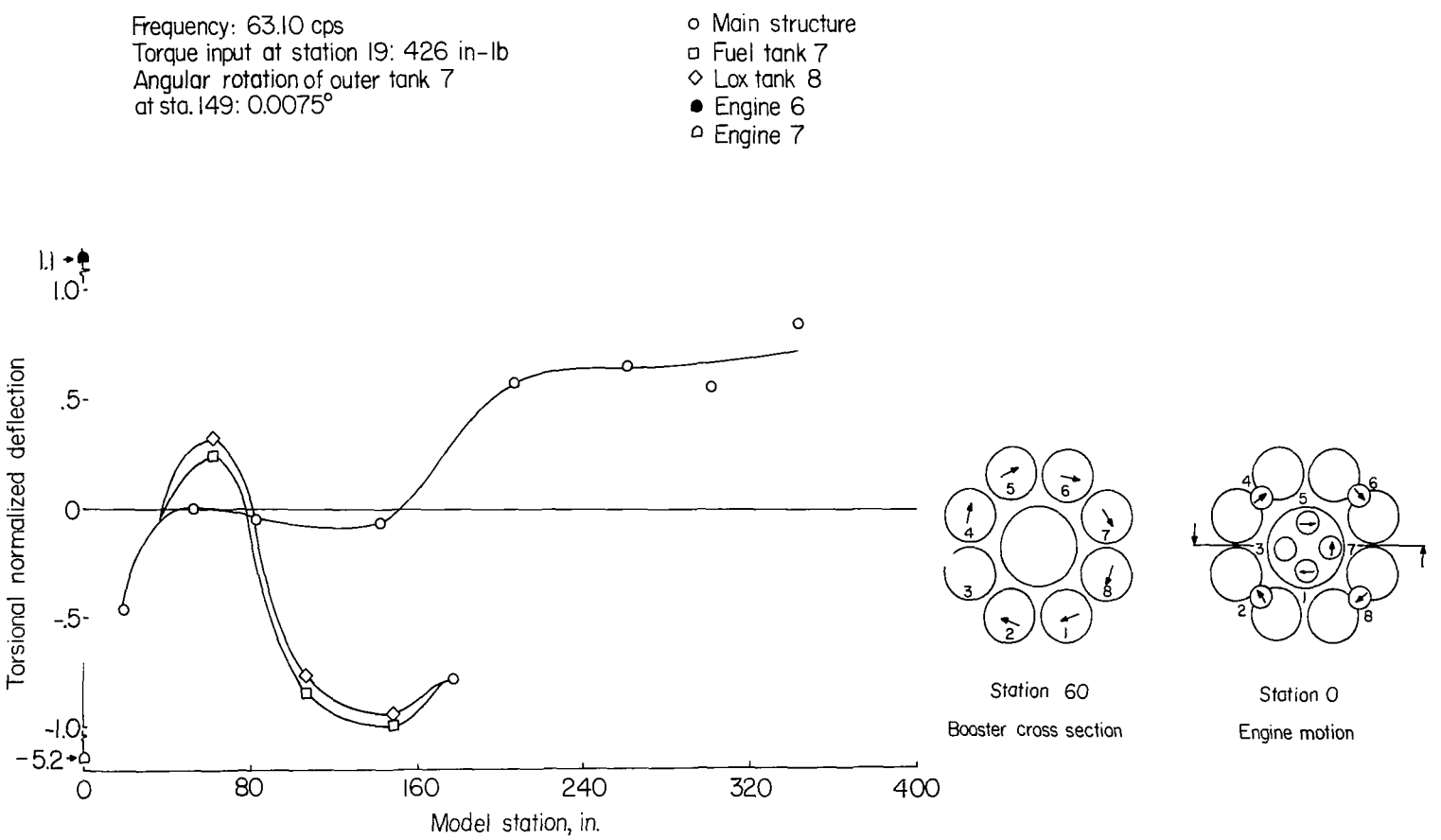

Figure 27.- Coupled first torsion, outer-tank second bending mode. Spring suspension; booster 48 percent full.

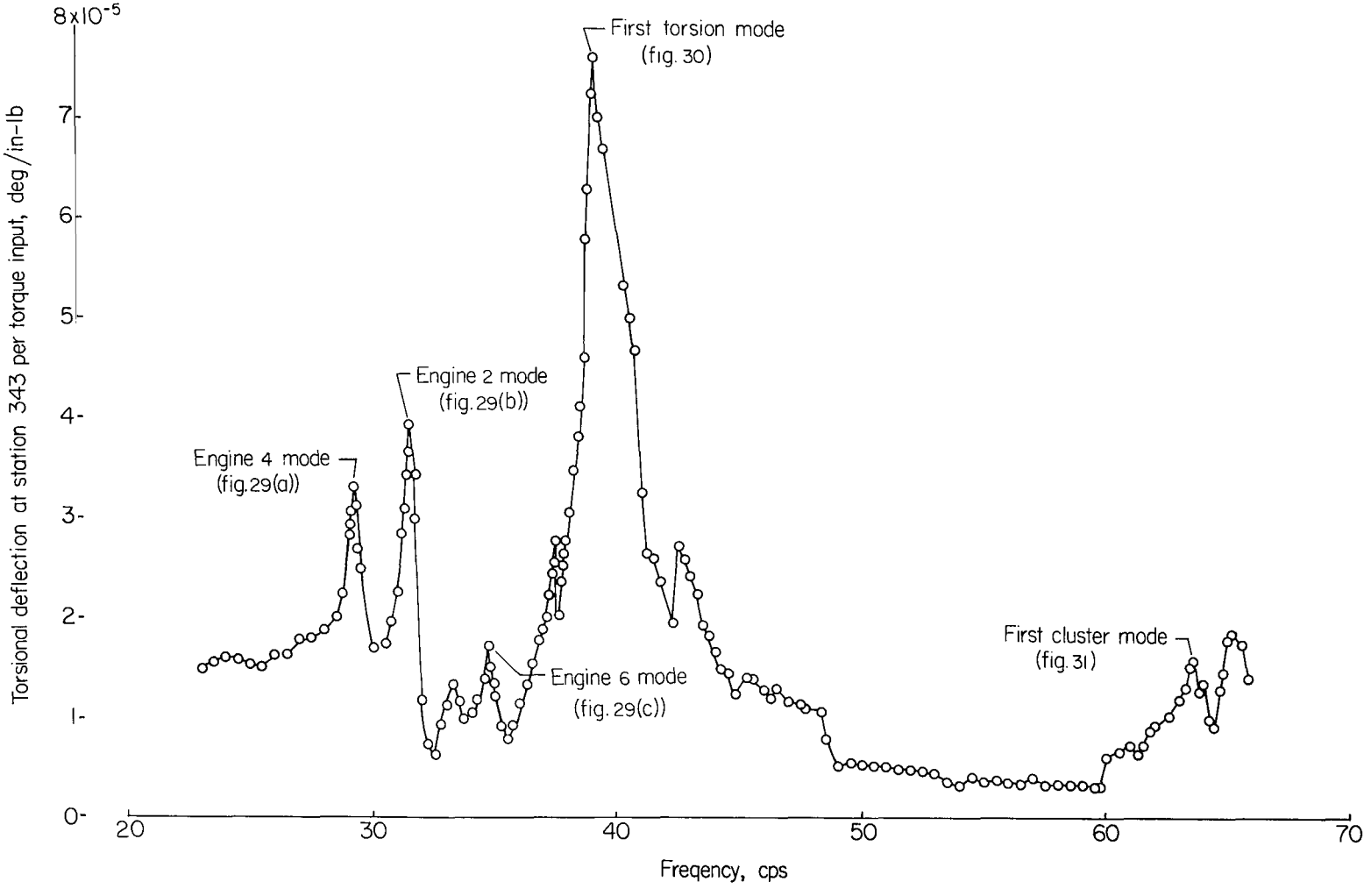

Figure 28.- Frequency response at station 343. Spring suspension; booster empty.

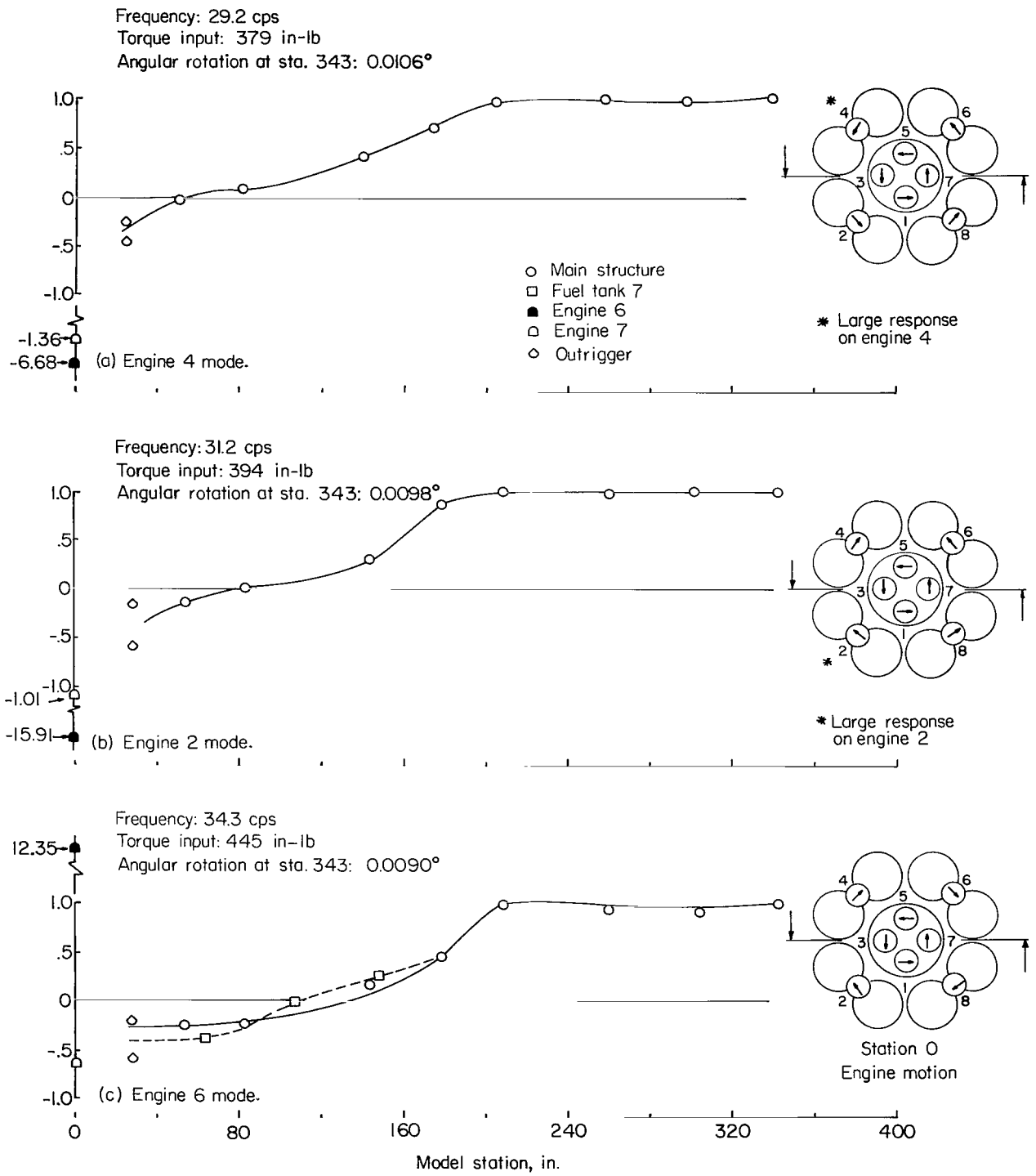

Figure 29.- Engine frequency modes. Spring suspension; booster empty.

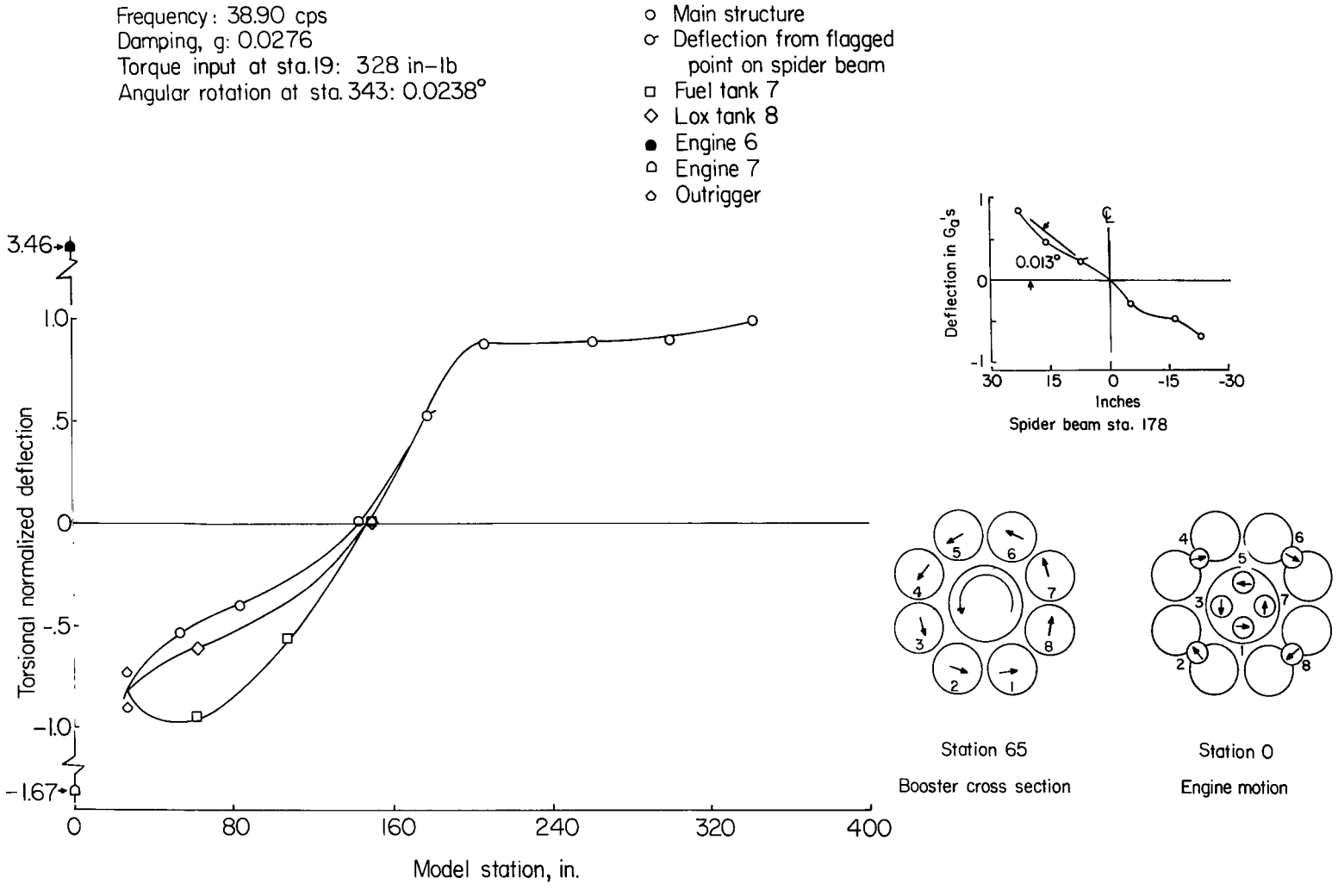

Figure 30.- First torsion mode. Spring suspension; booster empty.

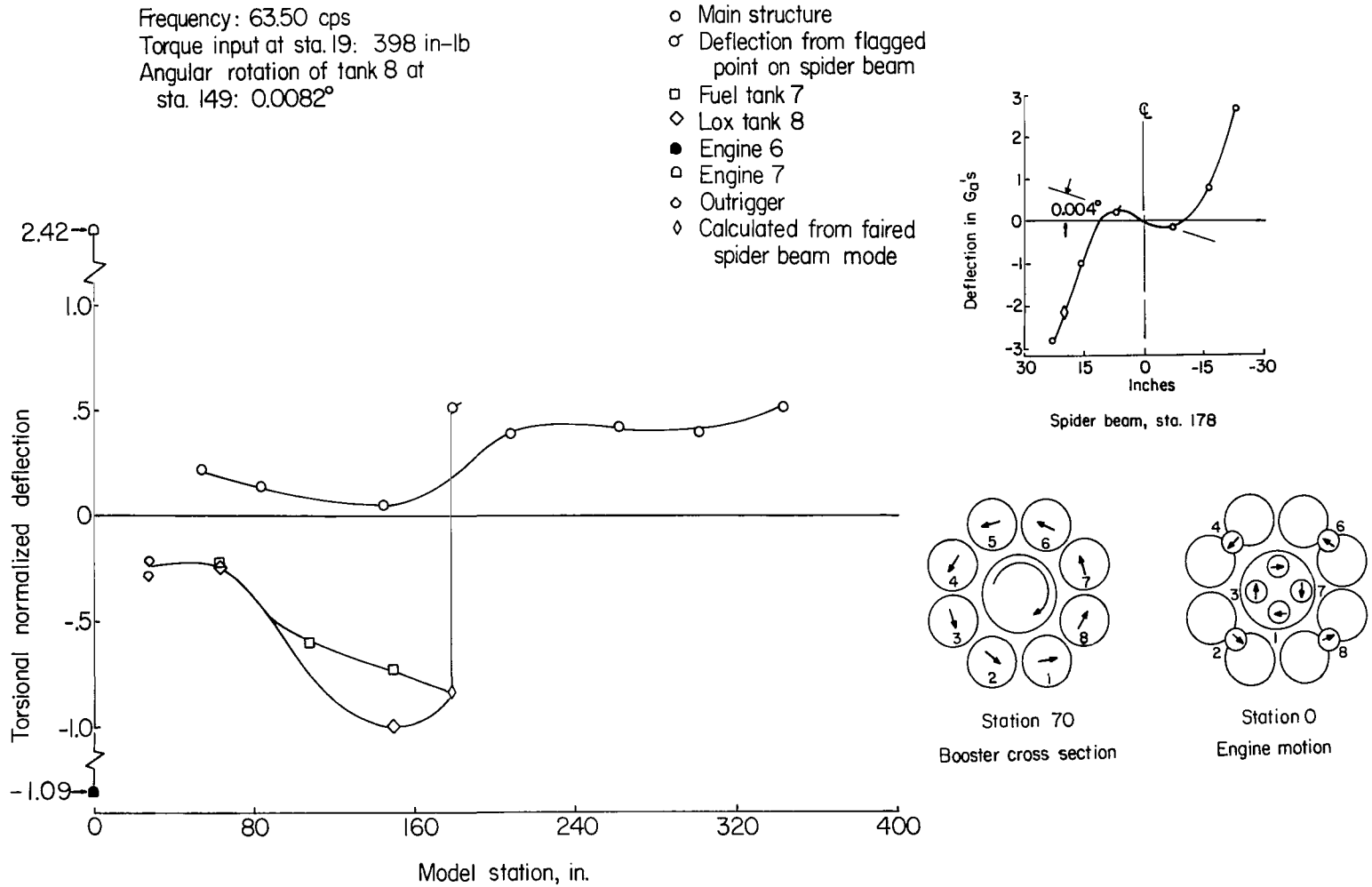

Figure 31.- First cluster mode. Spring suspension; booster empty.

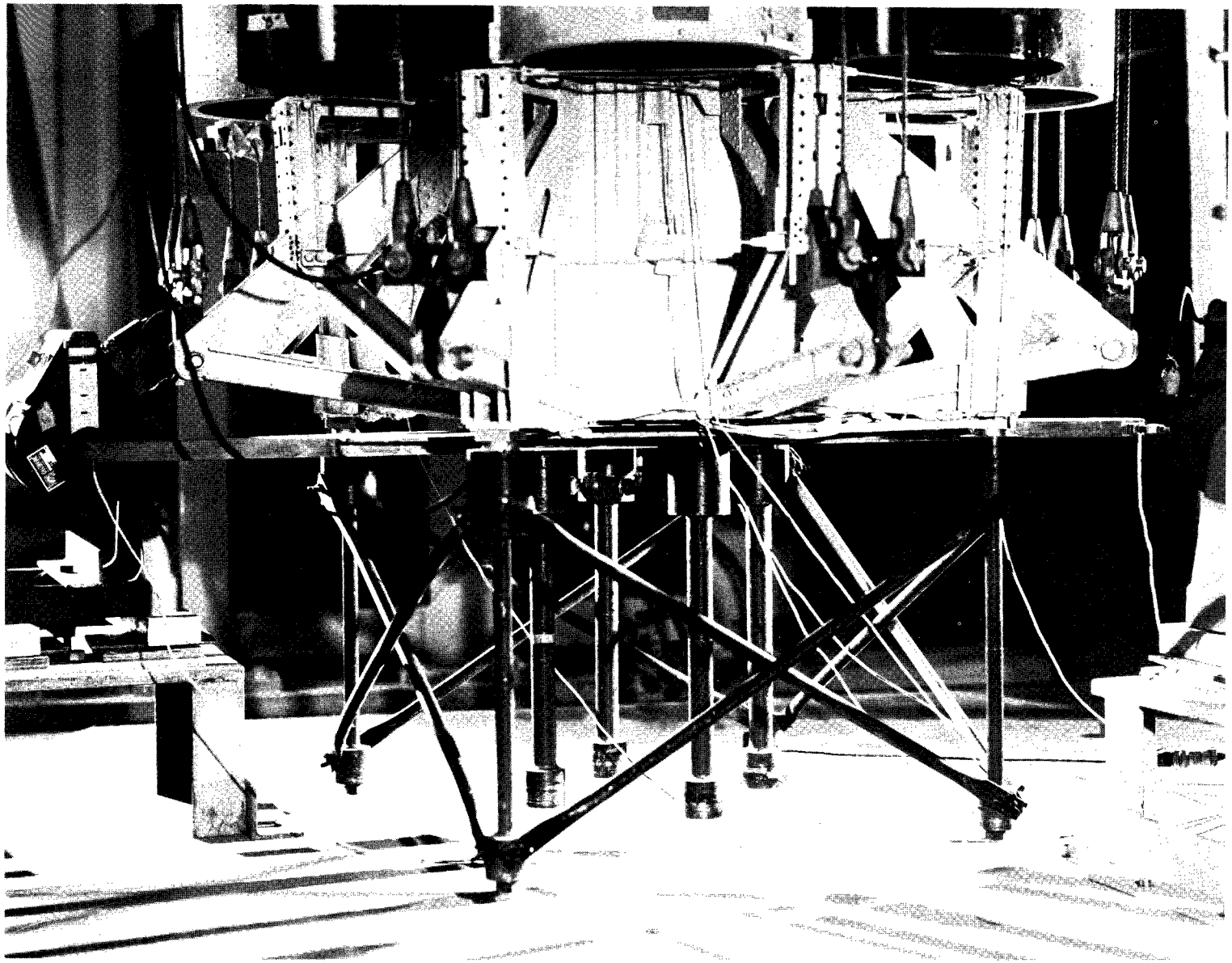

Figure 32.- Outboard engines braced. L-63-5449

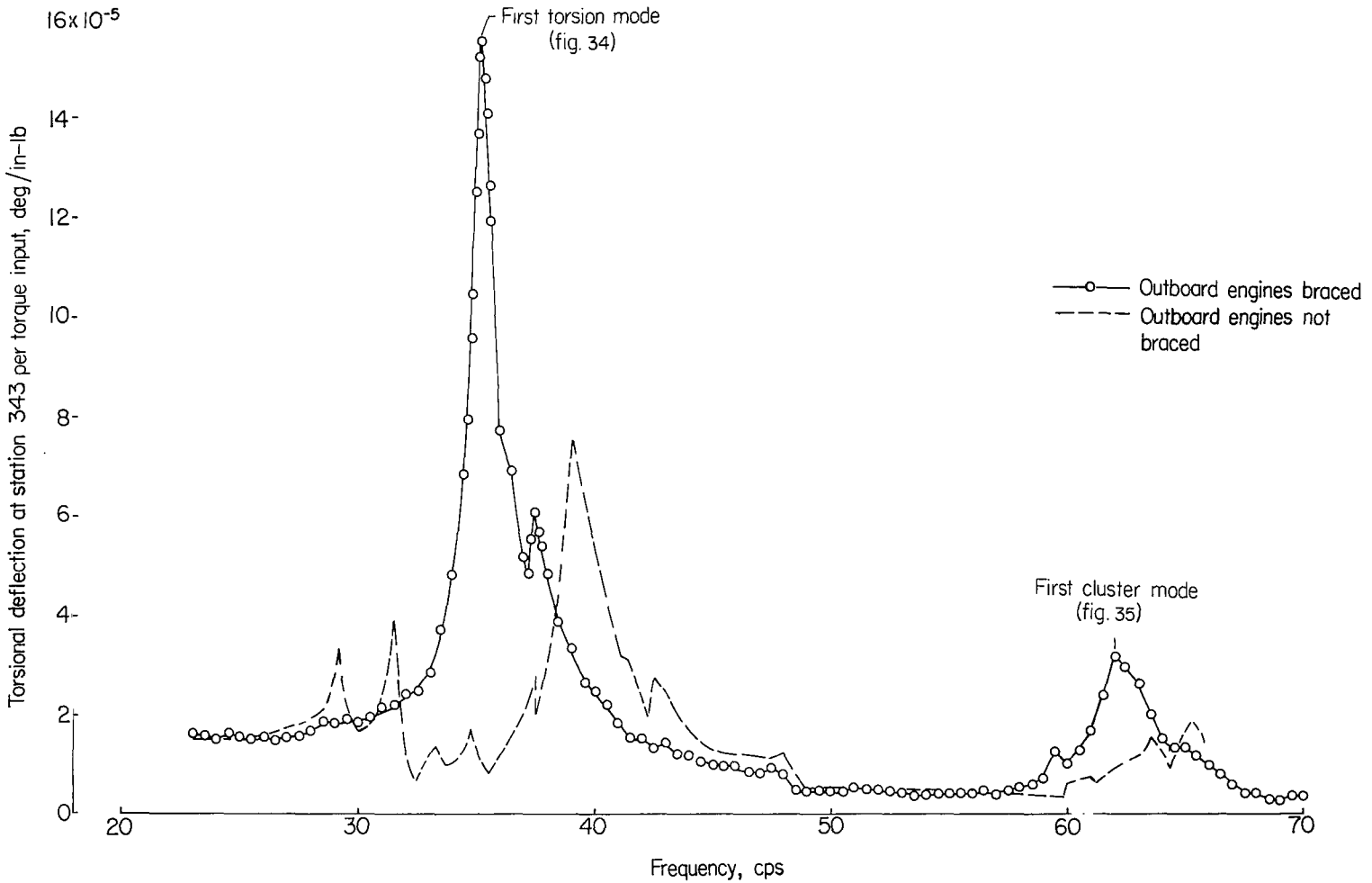

Figure 33.- Comparison of frequency response at station 343 with and without engines braced. Spring suspension; booster empty.

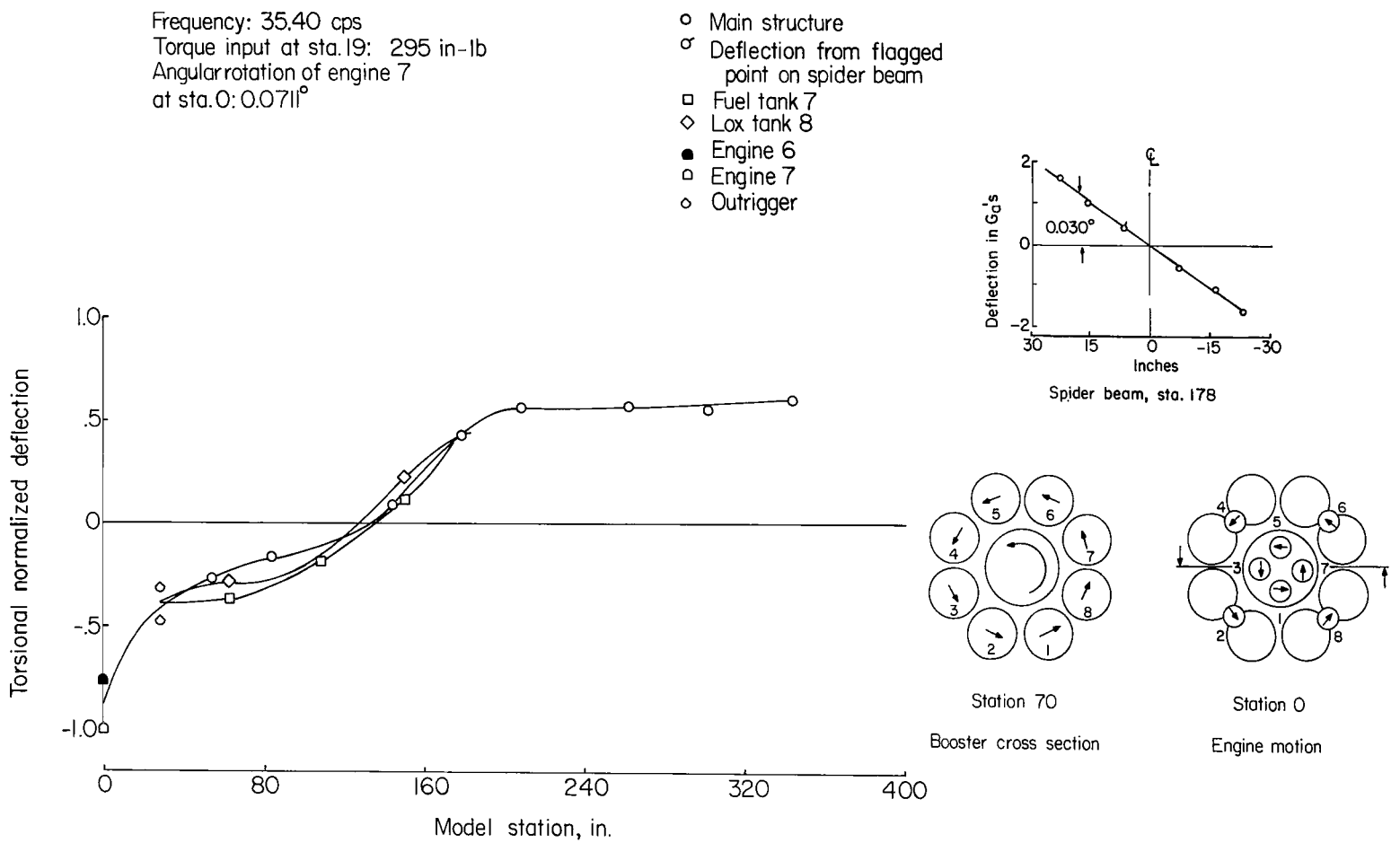

Figure 34.- First torsion mode with engines braced. Spring suspension; booster empty.

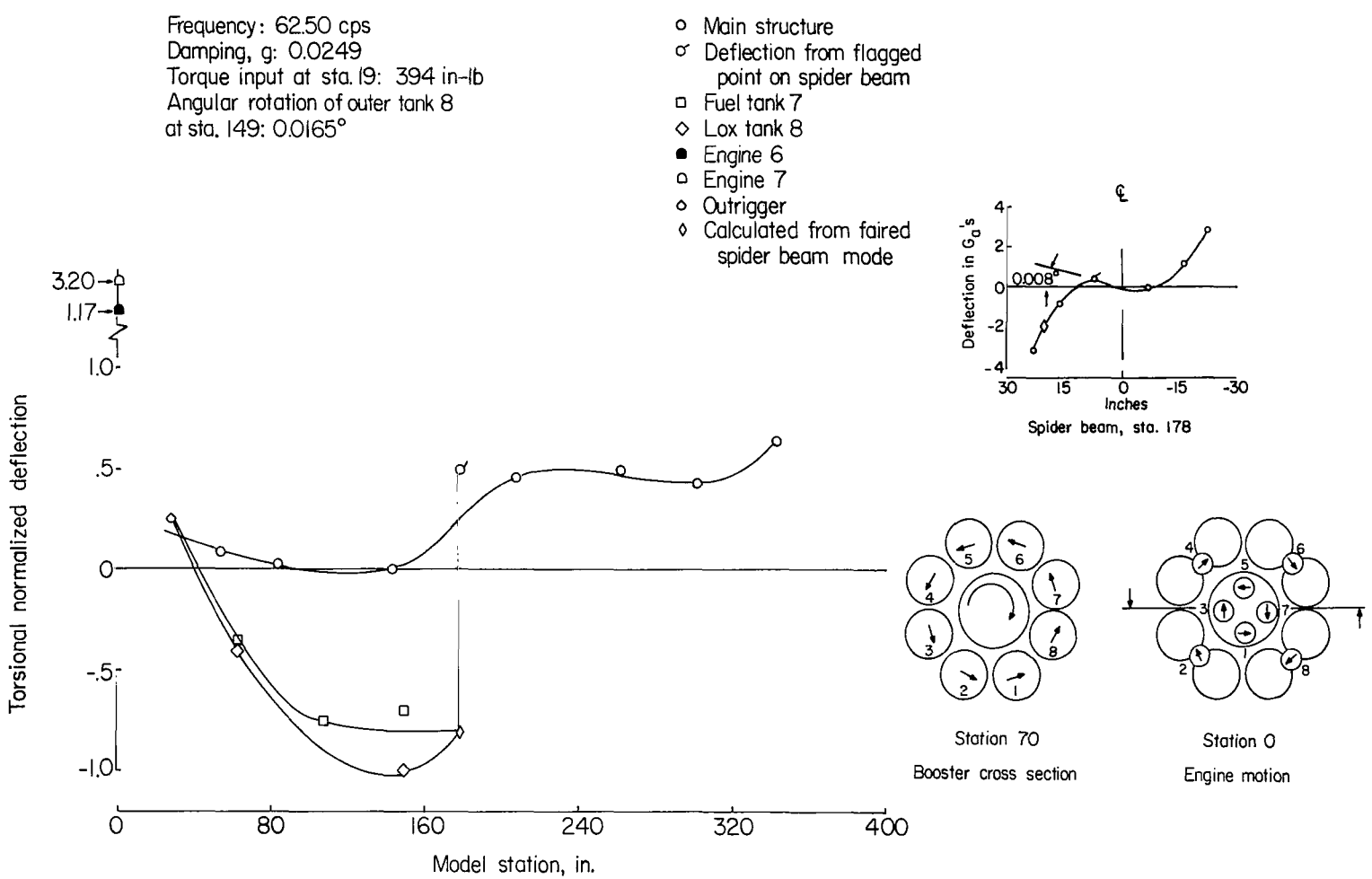

Figure 35.- First cluster mode with engines braced. Spring suspension; booster empty.

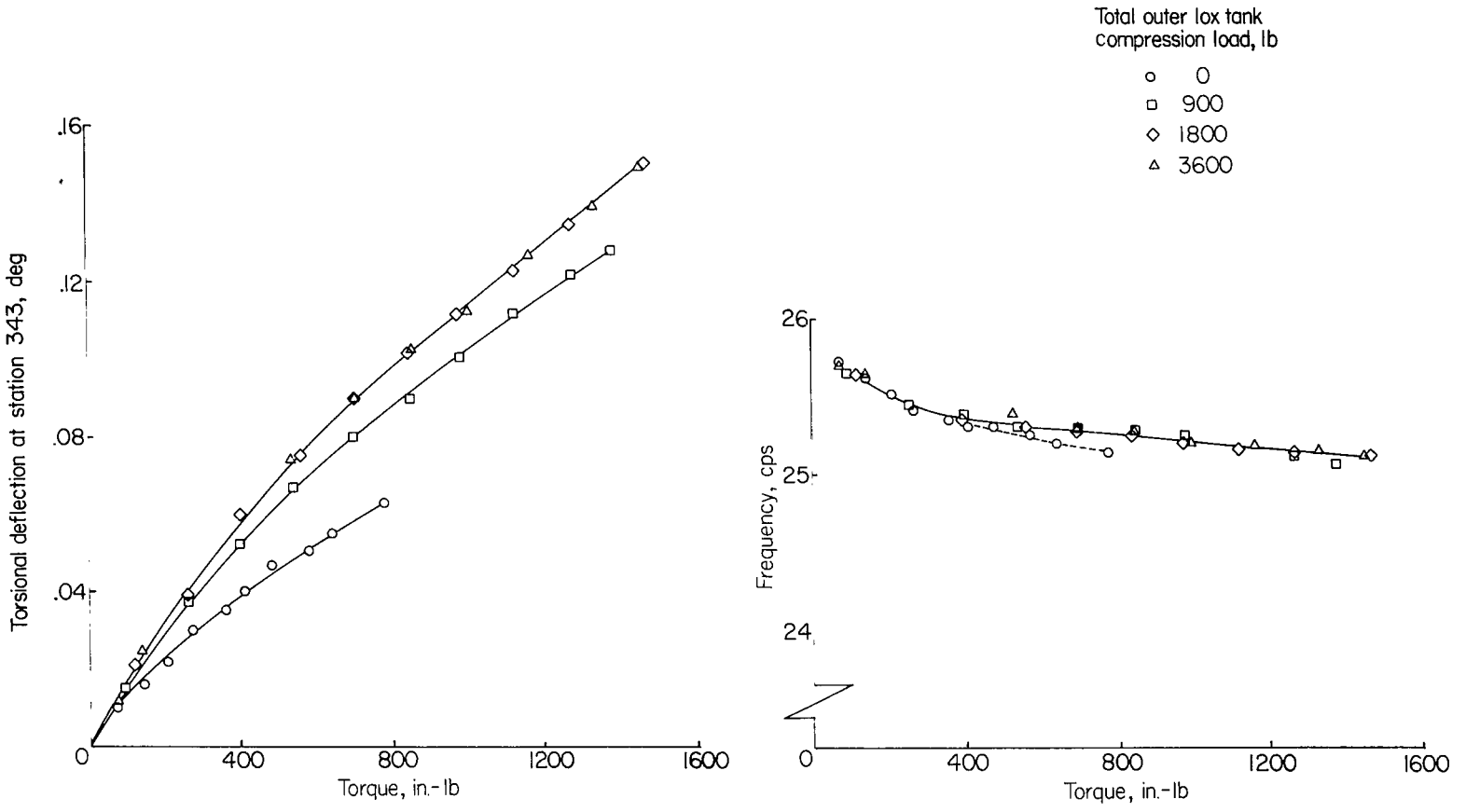

(a) Torsional deflection against torque input.

(b) Frequency against torque input.

Figure 36.- Variation of resonant frequency and amplitude with increased torque at first torsion mode. Spring suspension; booster full.

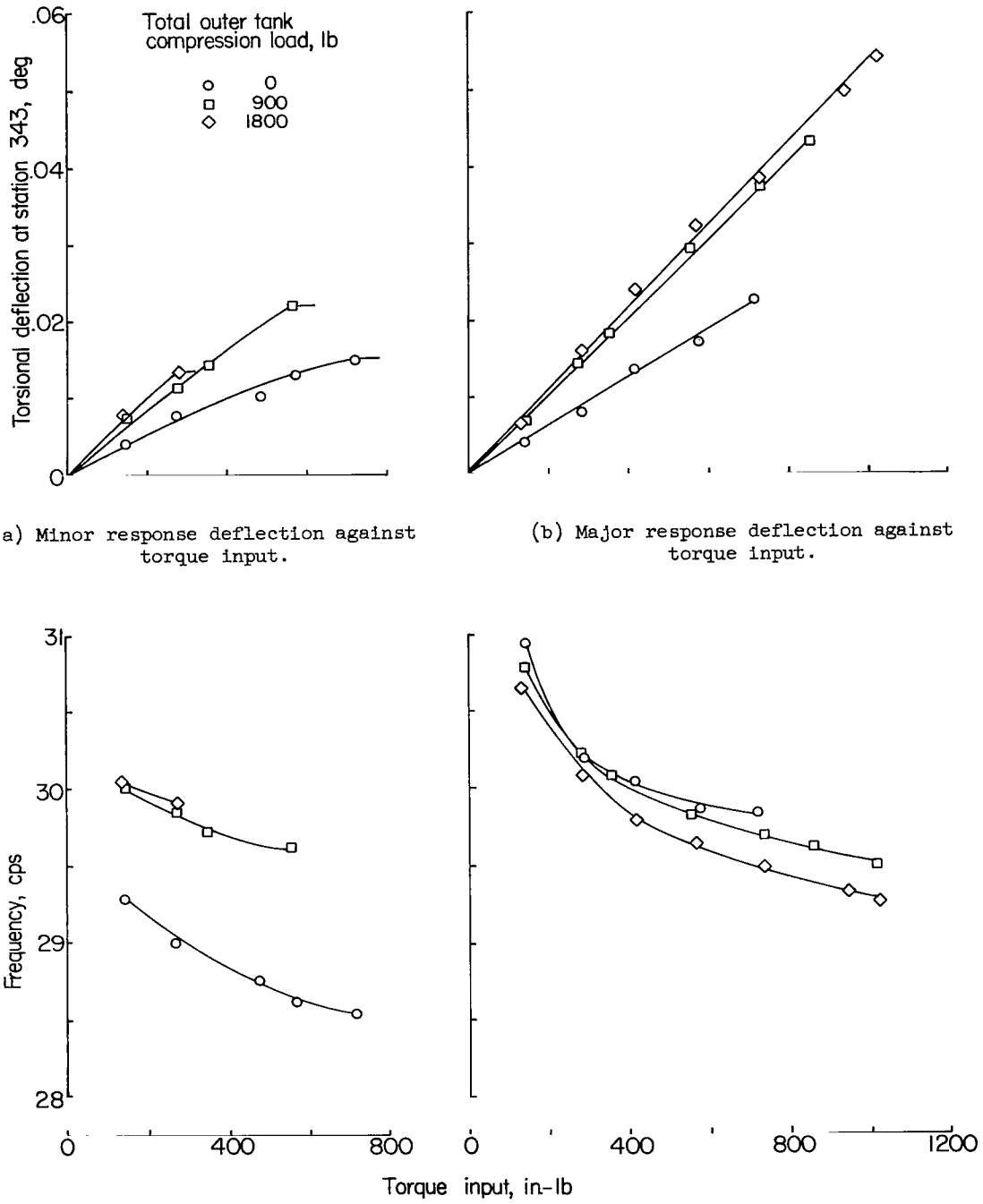

(a) Minor response deflection against torque input.

(b) Major response deflection against torque input.

(c) Resonant frequency of minor response against torque input.

(d) Resonant frequency of major response against torque input.

Figure 37.- Variation of double response peak with increased torque input. Booster 48 percent full.

2/22/85

"The aeronautical and space activities of the United States shall be conducted so as to contribute . . . to the expansion of human knowledge of phenomena in the atmosphere and space. The Administration shall provide for the widest practicable and appropriate dissemination of information concerning its activities and the results thereof."

—NATIONAL AERONAUTICS AND SPACE ACT OF 1958

NASA SCIENTIFIC AND TECHNICAL PUBLICATIONS

TECHNICAL REPORTS: Scientific and technical information considered important, complete, and a lasting contribution to existing knowledge.

TECHNICAL NOTES: Information less broad in scope but nevertheless of importance as a contribution to existing knowledge.

TECHNICAL MEMORANDUMS: Information receiving limited distribution because of preliminary data, security classification, or other reasons.

CONTRACTOR REPORTS: Technical information generated in connection with a NASA contract or grant and released under NASA auspices.

TECHNICAL TRANSLATIONS: Information published in a foreign language considered to merit NASA distribution in English.

TECHNICAL REPRINTS: Information derived from NASA activities and initially published in the form of journal articles.

SPECIAL PUBLICATIONS: Information derived from or of value to NASA activities but not necessarily reporting the results of individual NASA-programmed scientific efforts. Publications include conference proceedings, monographs, data compilations, handbooks, sourcebooks, and special bibliographies.

Details on the availability of these publications may be obtained from:

SCIENTIFIC AND TECHNICAL INFORMATION DIVISION

NATIONAL AERONAUTICS AND SPACE ADMINISTRATION

Washington, D.C. 20546